

**Coupling of MASH-MORSE
Adjoint Leakages with Space-
and Time-Dependent Plume
Radiation Sources**

**C. O. Slater
J. M. Barnes
J. O. Johnson
J. P. Renier
R. T. Santoro**

DOCUMENT AVAILABILITY

Reports produced after January 1, 1996, are generally available free via the U.S. Department of Energy (DOE) Information Bridge.

Web site <http://www.osti.gov/bridge>

Reports produced before January 1, 1996, may be purchased by members of the public from the following source.

National Technical Information Service
5285 Port Royal Road
Springfield, VA 22161
Telephone 703-605-6000 (1-800-553-6847)
TDD 703-487-4639
Fax 703-605-6900
E-mail info@ntis.fedworld.gov
Web site <http://www.ntis.gov/support/ordernowabout.htm>

Reports are available to DOE employees, DOE contractors, Energy Technology Data Exchange (ETDE) representatives, and International Nuclear Information System (INIS) representatives from the following source.

Office of Scientific and Technical Information
P.O. Box 62
Oak Ridge, TN 37831
Telephone 865-576-8401
Fax 865-576-5728
E-mail reports@adonis.osti.gov
Web site <http://www.osti.gov/contact.html>

This report was prepared as an account of work sponsored by an agency of the United States Government. Neither the United States Government nor any agency thereof, nor any of their employees, makes any warranty, express or implied, or assumes any legal liability or responsibility for the accuracy, completeness, or usefulness of any information, apparatus, product, or process disclosed, or represents that its use would not infringe privately owned rights. Reference herein to any specific commercial product, process, or service by trade name, trademark, manufacturer, or otherwise, does not necessarily constitute or imply its endorsement, recommendation, or favoring by the United States Government or any agency thereof. The views and opinions of authors expressed herein do not necessarily state or reflect those of the United States Government or any agency thereof.

Computational Physics and Engineering Division

Coupling of MASH-MORSE Adjoint Leakages with Space- and Time-Dependent Plume Radiation Sources

C. O. Slater
J. M. Barnes
J. O. Johnson
J.-P. Renier
R. T. Santoro

Date Published: April 2001

Prepared by the
OAK RIDGE NATIONAL LABORATORY
Oak Ridge, TN 37831-6363
Managed by
UT-BATTELLE, LLC,
for the

U.S. DEPARTMENT OF ENERGY
under contract DE-AC05-00OR22725

CONTENTS

	Page
LIST OF TABLES	v
LIST OF FIGURES	ix
ABSTRACT	xi
1.0 INTRODUCTION	1
2.0 RIGOROUS METHOD — COUPLING INDIRECTLY WITH PLUME SOURCES	3
2.1 Description	3
2.2 Testing of the Method	3
2.2.1 Test Case 1	3
2.2.1.1 Source	3
2.2.1.2 Building	4
2.2.1.3 Calculations	4
2.2.1.4 Results	5
2.2.2 Test Case 2	5
2.2.2.1 Source	5
2.2.2.2 Building	6
2.2.2.3 Calculations	6
2.2.2.4 Results	6
2.2.2.5 Sensitivity	7
2.2.2.6 GENMASH vs TORT Free-Field Dose Rates	8
2.2.2.7 Computation Time	8
2.2.3 Test Case 3	8
2.2.3.1 Source	8
2.2.3.2 Building	8
2.2.3.3 Calculations	8
2.2.3.4 Results	9
3.0 APPROXIMATE METHOD — COUPLING DIRECTLY WITH PLUME SOURCES ..	11
3.1 Description	11
3.2 Testing of the Method	13
3.3 Comparison of DRC4 and GENMASH Free-Field Dose Rates	15
4.0 CONCLUSIONS	17

5.0 REFERENCES	19
APPENDIX A. INPUT INSTRUCTIONS FOR VARIOUS CODES	65
A.1 Input Instructions for DRC4	67
A.2 Input Instructions for GENTORT	72
A.3 Input Instructions for PLATEQ	74
A.4 Input Instructions for VIST3DP	76
A.5 Input Instructions for QUAD3D	77
A.6 Input Instructions for G2GAIR	78
APPENDIX B. DESCRIPTIONS OF FILES USED OR CREATED BY VARIOUS CODES .	81
B.1 DRC4 Directional Fluence File Format	83
B.2 GENMASH Source File Format	84
B.3 GENTORT Output File Format	85
B.4 QUAD3D Output File Format	91
B.5 G2GAIR Output File Format	92
B.6 PLATEQ Output File Format	93
B.7 VIST3DP Scalar Fluence File Format	94
B.8 VIST3DP Directional Fluence File Format	96

LIST OF TABLES

Table	Page
1. Atomic Densities ($b^{-1} \text{ @cm}^{-1}$) of Elements in Mixtures Used in the Test Calculations	21
2. Extent of Structures in the Geometry for TORT/DRC3SRF Test Problem1	23
3. Comparison of Dose Rates for Forward-Forward (TORT-TORT) and Forward-Adjoint (TORT-MASH) Couplings	24
4. Energy Boundaries for the Photon Group Structures Used in the Calculations	25
5. ANSI Standard Photon Dose Rates (rem/h) at Detector Locations Inside a Two-Story Concrete Building	26
6. ANSI Standard Free-Field Photon Dose Rates (rem/h) at Detector Locations Inside a Two-Story Concrete Building	27
7. ANSI Standard Photon Dose-Rate Protection Factors at Detector Locations Inside a Two-Story Concrete Building	28
8. Comparisons of TORT and GENMASH Free-Field Dose Rates at X=-8.0875 km, Y=55 m, and Z=7.7004 m.	29
9. TORT/DRC3SRF Free-Field Fluence and Dose Rate and Protection Factors at a Corner Detector Position in a Large, Thin-Walled Building for a Plume Photon Source at Several Time Intervals (Coupled neutron and photon adjoint)	30
10. TORT/DRC3SRF Free-Field Fluence and Dose Rate and Protection Factors at a Center Detector Position in a Large, Thin-Walled Building for a Plume Photon Source at Several Time Intervals (Coupled neutron and photon adjoint)	31
11. TORT/DRC3SRF Free-Field Fluence and Dose Rate and Protection Factors at a Corner Detector Position in a Large, Thin-Walled Building for a Plume Photon Source at Several Time Intervals (Photon only adjoint)	32
12. Free-Field Fluence and Dose Rate and Protection Factors at a Center Detector Position in a Large, Thin-Walled Building for a Plume Photon Source at Several Time Intervals (Photon only adjoint)	33
13. Descriptions of the 3-D Quadrature Sets on the File Created by QUAD3D	34
14. Free-Field Data and Protection Factors for a Detector at Position 1 in a Two-Story Building. The DRC4 calculation used a 22-angle 1-D quadrature and an S_8 3-D quadrature to bin the 3-D fluences at eight fluence points surrounding the building for each time step (calculation time \sim 23 min. for two time steps	35
15. Free-Field Data and Protection Factors for a Detector at Position 2 in a Two-Story Building. The DRC4 calculation used a 22-angle 1-D quadrature and an S_8 3-D quadrature to bin the 3-D fluences at eight fluence points surrounding the building for each time step (calculation time 1.2 min. For two time steps because of time savings from the Table 1 calculations)	36

16. Free-field fluences ($\text{cm}^{-2} \text{ @ s}^{-1}$) and dose rates (rem/h) for detector 1 in a two-story concrete building (icbrt=2^a ; nrad=43^a ; DABL69 23-group photon structure; time=38.8 min)	37
17. Free-field fluences ($\text{cm}^{-2} \text{ @ s}^{-1}$) and dose rates (rem/h) for detector 1 in a two-story concrete building (icbrt=2^a ; nrad=82^a ; SCALE 18-group photon structure; time=34.2 min)	38
18. Free-field fluences ($\text{cm}^{-2} \text{ @ s}^{-1}$) and dose rates (rem/h) for detector 1 in a two-story concrete building (icbrt=2^a ; nrad=43^a ; SCALE 18-group photon structure; time=34.1 min)	39
19. Free-field fluences ($\text{cm}^{-2} \text{ @ s}^{-1}$) and dose rates (rem/h) for detector 1 in a two-story concrete building (icbrt=3^a ; nrad=43^a ; DABL69 23-group photon structure; time=132.5 min)	40
20. Free-field fluences ($\text{cm}^{-2} \text{ @ s}^{-1}$) and dose rates (rem/h) for detector 1 in a two-story concrete building (icbrt=3^a ; nrad=82^a ; SCALE 18-group photon structure; time=116.2 min)	41
21. Free-field fluences ($\text{cm}^{-2} \text{ @ s}^{-1}$) and dose rates (rem/h) for detector 1 in a two-story concrete building (icbrt=3^a ; nrad=43^a ; SCALE 18-group photon structure; time=116.0 min)	42
22. Comparison of TORT-DRC3SRF and DRC4 Fluences and Protection Factors for an Off-Center Detector in the Ten-Story NGIC Building D (includes roof source contribution; air attenuation by a 23-group photon library; attenuation data given for 43 distances)	43
23. Comparison of TORT-DRC3SRF and DRC4 Fluences and Protection Factors for a Centered Detector in the Ten-Story NGIC Building D (includes roof source contribution; air attenuation by a 23-group photon library; attenuation data given for 43 distances)	44
24. Comparison of TORT-DRC3SRF and DRC4 Fluences and Protection Factors for an Off-Center Detector in the Ten-Story NGIC Building D (includes roof source contribution; air attenuation by an 18-group photon library; attenuation data given for 82 distances)	45
25. Comparison of TORT-DRC3SRF and DRC4 Fluences and Protection Factors for a Centered Detector in the Ten-Story NGIC Building D (includes roof source contribution; air attenuation by an 18-group photon library; attenuation data given for 82 distances)	46
26. Comparison of TORT-DRC3SRF and DRC4 Fluences and Protection Factors for an Off-Centered Detector in the Ten-Story NGIC Building D (includes roof source contribution; air attenuation by an 18-group photon library; attenuation data given for 43 distances)	47
27. Comparison of TORT-DRC3SRF and DRC4 Fluences and Protection Factors for a Centered Detector in the Ten-Story NGIC Building D (includes roof source	

contribution; air attenuation by an 18-group photon library; attenuation data given for 43 distances)	48
28. Comparison of fluences and dose rates calculated by special codes using GENMASH sources, the DRC4 source-integration procedure, and ANISN air-attenuated angular fluences in two group structures	49
29. Comparison of GENMASH dose rates with TORT, DRC4, and Test Program dose rates	50

LIST OF FIGURES

Figure	Page
1. Exterior view of the two-story concrete building used in DRC3SRF and DRC4 test cases	51
2. Exterior view of the roofless two-story concrete building used in the DRC3SRF and DRC4 test cases	52
3. X-Y planar slice through building to show X-Y locations of detectors within the building. The first- and second-floor detectors have the same X and Y coordinates	53
4. Surface plot of the energy-integrated source ($\text{m}^{-3} \text{ @ s}^{-1}$) at 1-m height one hour after the start of a PWR accident	54
5. Surface plot of the energy-integrated source ($\text{m}^{-3} \text{ @ s}^{-1}$) at 1-m height three hours after the start of a PWR accident	55
6. 1-D airborne plume plus ground radiation source distribution as a function of distance along the X-axis	56
7. 1-D ground radiation source distribution as a function of distance along the X-axis	57
8. Geometry for the Large, Ten-Story, Thin-Walled, Concrete Building	58
9. Group 1 fluence spatial distribution as a function of quadrature and point source size	59
10. X-Y plane illustration of the original mesh used to integrate plume and surface source contributions to a point at the center of the center box (subdivisions of the first twelve annular regions are shown)	60
11. X-Y plane illustration of the revised coarser mesh used to integrate plume and surface source contributions to a point at the center of the center box (subdivisions of the first eight annular regions are shown)	61
12. Comparison of DRC3SRF and DRC4 free-field fluence spectra at detector position 1 in a two-story building for two time steps	62
13. Comparison of DRC3SRF and DRC4 shielded fluence spectra at detector position 1 in a two-story building for two time steps	63

ABSTRACT

In the past, forward-adjoint coupling procedures in air-over-ground geometry have typically involved forward fluences arising from a point source a great distance from a target or vehicle system. Various processing codes were used to create localized forward fluence files that could be used to couple with the MASH-MORSE adjoint leakages. In recent years, radiation plumes that result from reactor accidents or similar incidents have been modeled by others, and the source space and energy distributions as a function of time have been calculated. Additionally, with the point kernel method, they were able to calculate in relatively quick fashion free-field radiation doses for targets moving within the fluence field or for stationary targets within the field, the time dependence for the latter case coming from the changes in position, shape, source strength, and spectra of the plume with time. The work described herein applies the plume source to the MASH-MORSE coupling procedure. The plume source replaces the point source for generating the forward fluences that are folded with MASH-MORSE adjoint leakages.

Two types of source calculations are described. The first is a "rigorous" calculation using the TORT code and a spatially large air-over-ground geometry. For each time step desired, directional fluences are calculated and are saved over a predetermined region that encompasses a structure within which it is desired to calculate dose rates. Processing codes then create the surface fluences (which may include contributions from radiation sources that deposit on the roof or plateout) that will be coupled with the MASH-MORSE adjoint leakages. Unlike the point kernel calculations of the free-field dose rates, the TORT calculations in practice include the effects of ground scatter on dose rates and directional fluences, although the effects may be underestimated or overestimated because of the use of necessarily coarse mesh and quadrature in order to reduce computational times. The second source calculation uses a point kernel like method to calculate directional fluences at points surrounding user-specified detector and structure locations and folds those fluences with MASH-MORSE adjoint leakages to calculate free-field and shielded fluences and dose rates and the indicated protection factors.

Both source calculation methods were tested for determining dose rates at specified locations within a two-story concrete building. For two early time steps, results from the second method are 50 to 60% higher than those from the first method, but the protection factors differ by only a few percent. This indicates that the free-field and shielded fluence spectra are similar and differ mainly in magnitude. Other comparisons were made, and from the comparisons there was a perceived underprediction by TORT. That underprediction can be attributed to the coarse mesh and quadrature used in the calculations. The second method, while not rigorously correct, requires much less computer time for a reasonably good estimate of the shielded dose rates within a structure.

1.0 INTRODUCTION

For a span of more than thirty-five years,¹⁻⁸ much effort has been expended toward the calculation of shielded fluences, dose rates, or reaction rates within so-called “targets” such as buildings, armored vehicles, and other structures or objects due to point radiation sources situated in low-density media (usually air, air-over-ground, or void in the case of Ref. 1) at large distances from the objects. It has been found that economical solutions can be obtained by separating the problem into three parts. In the first part, the geometry is simplified by removal of the target from the geometry, and a source calculation is performed with a two- or three-dimensional discrete ordinates code starting from a first-collision source file. For the case of a target in air-over-ground medium, only air and ground media are included in the geometry for this problem. For the point source, this calculation yields space-dependent free-field fluences for each group in the chosen energy range. Also included in this part of the calculation is the preparation of the equivalent source file and other files that will be used in the third part of the problem. In the second part of the problem, an adjoint Monte Carlo calculation is performed in a localized and generally complex geometry. The adjoint source consists of a point source at the detector location and each energy group has a source strength of 1.0. Any response function (adjoint source spectra) may be used, but the unit source in each group allows for more uniform sampling in energy. For each leakage event, both the source and leakage energy group numbers are written along with other parameters to an event file. This enables the calculation of differential spectra along with integral quantities at the detectors. The third part of the problem (the coupling calculation) determines the correspondences between the calculations in the first and second parts of the problem (i.e. the spatial offsets and orientations) and folds the forward fluences and adjoint leakages to calculate the shielded detector response. Then shielding protection and reduction factors are calculated based on the free-field and shielded dose rates at the detector. The initial coupling code, DRC,⁵ used directional fluences that varied only in one spatial dimension. Subsequent extensions of the code added more detailed spatial representation of the directional fluences. These code extensions accommodated the newer methods and retained the DRC method through the use an input parameter **idos** that causes the appropriate parallel coding to be executed.

Recently, studies of the airborne transport of radiation plumes and the free-field dose rates that result therefrom have been conducted. A series of codes⁹ is used to model radiation dispersal in plumes resulting from nuclear accidents of various origins (such as reactors, nuclear processing plants, and weapons). Sources (mainly photons) resulting from airborne and ground-deposited radioisotopes are combined by the GENMASH code¹⁰ into energy groups, and source arrays are created as functions of time, space, and energy. These data can then be integrated in point kernel fashion to give free-field dose rates at selected locations. Unfortunately, the energy spectrum at the detector is not obtained when the point kernel method is used. This was identified as a problem when a desire was expressed for using the plume source in place of the point sources previously used in air-over-ground forward-adjoint coupling calculations. Two methods, one rigorous and one approximate, were developed for implementing the plume source in the coupling scheme.

Section 2.0 describes the rigorous method developed initially and results for test problems, while Section 3.0 describes the less time-consuming approximate method. Section 4.0 presents the conclusions. In addition, appendices include input descriptions for the various codes and the file formats used or created by the various codes.

2.0 RIGOROUS METHOD -- COUPLING INDIRECTLY WITH PLUME SOURCES

2.1 Description

The rigorous method of solving a problem with a plume source required an alteration of the form of the forward fluence file that one inputs to the coupling code. First, the general nature of the plume source necessitates that a three-dimensional (3-D) discrete ordinates calculation be performed to obtain the free-field fluences. The TORT 3-D discrete ordinates radiation transport code¹¹ was used for these source calculations. The GENTORT code¹² was used to prepare the source input for the TORT code from the GENMASH distributions. The energy structure of the source was changed from that of GENMASH to that of TORT. Postprocessing codes TORSET¹³, PLATEQ¹⁴, and VIST3DP¹⁵ were used to prepare directional fluence files (with or without plateout on the top of the structure) and free-field fluence files needed for the coupling calculation. Because of the large file that would result if fluences were saved for all the TORT mesh points, the mesh for which the directional fluences were output by TORT were confined to a relatively small patch region of the geometry. A second calculation, a MASH-MORSE adjoint Monte Carlo calculation that is the same for both the rigorous and approximate methods, was also performed. The coupling calculation used the code DRC3SRF¹⁶ (altered from a previous folding code, DRC3⁸) to fold the forward fluences with the MASH-MORSE^{5,7,8} adjoint leakages. Since the TORT and MASH-MORSE energy group structures were different, it was necessary to change the source group structure from the TORT structure to the MASH-MORSE structure prior to coupling in DRC3SRF.

2.2 Testing of the Method

As stated above, the coupling calculation was performed using the DRC3SRF code, which includes several folding options selected by the input parameter “idos.” The DRC3SRF folding method (input parameter **idos=2**) was tested using three sample problems. For each problem, dose rates were determined for detector locations within multistory concrete buildings. The compositions of all the material mixtures appearing in the building geometries are given in Table 1.

2.2.1 Test Case 1

The method was first tested by comparing calculated shielded dose rates at ten locations within a two-story concrete building.

2.2.1.1 Source A fictitious plume source was used, and the spatial extent of that source is described in Table 2. The energy spectrum of the source was given by

$$s(E) = 1.4 \times 10^{11} \times e^{-1.1E}$$

where the photon energy, E , has units of MeV. The function $s(E)$ is easily integrated over the group energy bounds to give the source in each energy group:

$$\int_{E_1}^{E_2} s(E) dE = 1.273 \times 10^{11} \times (e^{-1.1E_1} - e^{-1.1E_2})$$

where E_1 and E_2 are respectively the lower and upper energy boundaries (MeV) of the energy group.

2.2.1.2 Building The dimensions of the two-story building extend from 0.0 to 1737.36 cm in the X direction, from 0.0 to 1463.04 cm in the Y direction, and from 50.0 to 640.08 cm in the Z direction (Z=0.0 cm is at ground level). The floors and roof consist of 10.16-cm-thick reinforced concrete slabs, the second floor and roof being supported by 10.16-cm-wide \times 30.48-cm-high reinforced concrete beams running along the X dimension. Each floor is divided into four offices and a central hallway that runs along the Y dimension. The walls are composed of 30.48-cm-thick masonry blocks and are represented in the model by reduced-density ordinary concrete. Each office has one window on each outside wall bordering it and a door along the interior hallway. The windows and doors are modeled with the same thicknesses as the walls. The windows are represented by low-density silicon dioxide and the doors are represented by a low-density steel material. Figure 1 shows a drawing of the building with the windows and doors pictured as void for easy viewing in the figure. Figure 2 shows the building with the roof removed, and Figure 3 shows a planar slice through the building and small rectangles at the X-Y coordinates of the selected detector positions (five on each floor). The detector X-Y coordinates are the same on both floors. The detector position labeled number 1 is in front of a window and was intended to be facing the source. However, because the source moves along the negative X axis, the detector is actually turned away from the source. Likewise, detector 2 is shielded by a wall and is away from the source. Detector 3 is in the hallway while detectors 4 and 5 are behind doors in adjacent offices and were intended to be the most heavily shielded locations away from the source. The detectors could have been oriented as intended through a 180E rotation of the TORT free-field geometry about the origin during the source calculation.

2.2.1.3 Calculations. A 15-photon-energy-group, $S_{10}P_3$ TORT free-field calculation was performed using the fictitious source, and ten 23-photon-group (DABL69¹⁷ group structure) MASH-MORSE adjoint calculations were performed, one for each detector location within the building. For each MASH-MORSE calculation, 2,000,000 histories were followed. Calculations of dose rates at detector locations within the building were performed by two methods. Both methods depend on TORT free-field fluences on exposed surfaces of the building. In the first method, a building calculation is performed using TORT and the free-field fluences described above. This is a TORT-forward to TORT-forward (TORT-TORT) coupled calculation. The secondary TORT calculation used an S_8 quadrature and P_3 Legendre polynomial expansions of the scattering cross sections. The second method couples TORT-forward free-field fluences to MASH-MORSE adjoint leakages (TORT-MASH); DRC3SRF performs the coupling for the latter method. Seventy TORT-MASH coupling cases were performed (seven time steps and 10 detectors). Boundary fluences from the TORT free-field calculation were converted to the 23-group structure (**idif=1**) in order to avoid rerunning the MASH-MORSE cases with the 15-group structure.

It was later discovered that some of the materials in the building were incorrectly placed in the geometry model in both the TORT and MASH-MORSE calculations. The air and ground mixtures were correct. However, the floors, roof, and supports should have been rebar concrete instead of portland concrete; the walls should have been concrete block instead of steel; and the door and window mixtures should have been those shown in Table 1 instead of rebar concrete and concrete blocks, respectively. So, while the problem solved was not the one intended, both TORT-TORT and TORT-MASH calculations were performed using the same incorrect materials. Hence, the results should be comparable.

2.2.1.4 Results. Comparisons were made of fluences and dose rates calculated using a forward-TORT to forward-TORT coupling (TORT-TORT) and those obtained using a forward-TORT to adjoint-MASH-MORSE coupling (TORT-MASH). The source (surface fluences) for the second TORT calculation in the TORT-TORT sequence was prepared in the same manner as the source was prepared for the TORT-MASH coupling except for the file header records and the number of spatial mesh points (fewer were needed in the TORT-MASH case because interpolation was used to calculate fluences at all other spatial locations). Coupling calculations were performed both with and without plateout sources on the roof of the building. The directional fluences due to plateout were calculated simply by dividing the source strength by the cosine between a given direction and the surface inward normal. Results are shown in Table 3. Except for two positions on the first floor, the agreement between results from the forward-forward and the forward-adjoint coupling is generally good to excellent. For the two results with the greatest disagreements (position 3 for sources A and B), similar results were obtained for building roof sources with or without the inclusion of plateout sources. Even some results with relatively large fractional standard deviations are in good agreement. In addition, the results show the effect from the roof plateout source to be up to 10% on the first floor and up to 25% on the second floor. Results from this problem provided assurance that the coupling procedure was correct and could be applied to a more realistic plume source.

2.2.2 Test Case 2

The next test of the coupling procedure involved a more realistic GENMASH plume source.

2.2.2.1 Source. The code GENTORT calculated TORT volumetric sources for each of the seven time steps characterizing the GENMASH source file. Input instructions for GENTORT are given in Appendix A. The GENMASH source for this test case was one due to a modeled hypothetical reactor accident lasting three hours, and the source file included data on the radiation distribution for several times after the accident initiation (1.0, 2.0, 3.0, 4.4, 5.8, 7.2, and 10.0 h). The GENMASH source geometry extended from -80 km to +1 km in X, from -6 km to +6 km in Y, and from 0 km to +0.2 km in Z. The accident occurred at the origin (X=0.0 and Y=0.0) with time-dependent releases between 0 and 3 hours. A strong unidirectional wind moved the radioactive materials downrange (i.e. along the negative X axis). The GENMASH group structure consisted of 18 photon groups¹⁸ with energies ranging from 10 keV to 14 MeV (see the third column of Table 4), and the source was regrouped into another photon 18-group

structure (TORT group structure¹⁹) shown in the fourth column of Table 4. Since there was no source in the energy range above 5.0 MeV, the top three groups of the TORT group structure were eliminated to produce a 15-group structure having a maximum energy of 5.0 MeV. Note that there is no source in the top five GENMASH groups which also have energies above 5.0 MeV. The TORT free-field geometry extended from -2 km to +2 km in X, from -1 km to +1 km in Y, and from -50.0 cm to +1 km in Z. The mesh consisted of $96 \times 55 \times 35$ mesh cells. The origin of the TORT system was placed at (-8.0 km, 0.0 km, 0.0 km) in the GENMASH geometry. The mesh-edge source file option was selected. Figures 4 and 5 show typical plume source distributions, and Figures 6 and 7 show one-dimensional distributions (integrated over two spatial dimensions) of the total and ground sources along the X direction. The airborne source, which is not shown separately in these figures, is high near the reactor location at $t=1.0$ h and shifts toward -80.0 km at later times and completely disappears between 5.8 h and 7.2 h after the accident. The ground source peaks initially near the reactor but is nearly uniform from -10.0 km to -80.0 km after 4.4 h.

2.2.2.2 Building. The building is the same as that described in Section 2.2.1 except for the corrections that were made in the material specifications in MASH-MORSE.

2.2.2.3 Calculations. TORT 15-photon-group free-field calculations were performed for the converted GENMASH sources at the seven time steps, and boundary fluences were saved at the surfaces of the building to be used later in coupling calculations. The TORT calculations were run using an S_8 symmetric quadrature, a 15-group photon energy structure ($E < 5.0$ MeV), and a P_3 Legendre polynomial expansion of the scattering cross sections. Following the completion of the TORT calculations, the directional fluence files were processed and optionally enhanced by contributions from roof plateout sources, and the adjoint leakages and forward fluences were folded together to give dose rates at the ten detector locations used in the previous test problem. Adjoint MASH-MORSE calculations were performed for ten detector locations within the building after the material specifications were corrected (see Section 2.2.1.2). These MASH-MORSE calculations used the same photon energy structure (15 groups) as that used in the TORT calculations. For each MASH-MORSE calculation, 2,000,000 photon source histories were followed. Seventy coupling cases were performed with DRC3SRF (seven time steps and 10 detectors). Calculation times were 725 to 800 min for the TORT calculations, 61 to 82 min for the MASH-MORSE calculations, and 0.25 to 0.5 min for the DRC3SRF coupling calculations. The TORSET and VIST3DP calculations that processed the output TORT boundary fluences (to be used by DRC3SRF) used a combined total of about 4.5 seconds.

2.2.2.4 Results. Photon dose rates inside the building as a function of time and detector position are shown in Table 5. The free-field dose rates (i.e. the dose rates that one calculates at the detectors in the absence of a building) are shown in Table 6, and the dose-rate protection factors are shown in Table 7. The dose rates show about the same trend for all detectors, rising slightly for the first three hours of the accident, falling somewhat more than two orders of magnitude about one hour after the accident stopped, and falling off slowly with time beyond 4.4 h. For the first floor, protection factors rise slightly during the first three hours of the accident, dip somewhat after shutdown, and slowly rise at later times. The

second-floor results are similar except the protection factors rise after shutdown instead of dipping as they did for the first-floor detectors. There are no independent results against which to compare these results. However, results from the first test problems give confidence that the results are reasonable.

2.2.2.5 Sensitivity. The sensitivity of the TORT calculations to the spatial extent of the source was tested. The TORT calculations were performed over a fraction of the GENMASH geometry, and the size needed for the TORT geometry was determined using one-dimensional calculations. In those calculations, an airborne source volume was added to a spherical geometry until the fluence at the center of the sphere stopped increasing. From those results, it was determined that 2×10^5 cm (2 km) of air with source was sufficient. Thus, the TORT geometry extended from -2 km to +2 km in X. For time step 1, an additional TORT calculation was run with the geometry extending from -3 km to +3 km in X. The maximum increase in the free-field dose rates was 0.0026%. Hence, the smaller TORT geometry was deemed to be of adequate size.

A second sensitivity study examined the effect of the perturbations made to the source in the region occupied by the building. Free-field and shielded dose rates were examined for perturbed and unperturbed source fields. If the perturbation of the source causes minor changes to the dose rates, then the free-field TORT calculations can be performed without consideration of the presence of the building or any other perturbation. The source perturbation was implemented by redistributing the source in the space occupied by the building mockup uniformly in the mesh cells surrounding the building and distributing the ground source as a volume source in the mesh cells in the plane above the roof. If the source perturbation can be ignored, then the ground source could easily be added to the roof boundary fluence prior to folding with the MASH-MORSE leakages. The comparisons of the shielded dose rates showed dose rates from the unperturbed field to be 2.2 to 8.3% lower on the first floor and 1.1 to 4.2% lower on the second floor. There is more source entering the building mockup in the perturbed case because about half of the isotropic source, redistributed into the intervals surrounding the building, is directed into the building. That increases the fluence that is folded with the MASH-MORSE leakages.

While shielded dose rates were all lower for the unperturbed field, the effects on the free-field fluences were mixed. For the location in the ground beneath the building mockup, the dose rate is about 10% higher for the unperturbed field. Dose rates in the ground away from the building mockup differ little. The dose rate at a point within the building mockup and slightly above the ground is about 9% higher for the unperturbed field. For locations just outside the building mockup, dose rates for the unperturbed field ranged from 2% lower to 7% higher, most likely due to the assumption of a uniform redistribution around the building rather than a distribution like that for the intervals well outside the mockup. Dose rates above the roof were 1.4% lower to 1.5% higher for the unperturbed field.

Overall, it appears that the unperturbed free-field fluences will be adequate for calculating dose rates within buildings. So, if enough directional fluences are retained (i.e. over a large enough spatial extent), dose rates within the building may be obtained for any positioning of the building that leaves it within the extent of the fluence field.

2.2.2.6 GENMASH vs TORT Free-Field Dose Rates. The GENMASH code calculates sources as well as dose rates due to those sources, and TORT uses reformatted GENMASH sources to calculate free-field fluences in an air-over-ground geometry. The dose-rate calculations performed by GENMASH use dose factors from *ICRP Publication 51*²⁰ and "Geometric Progression Gamma-Ray Exposure Buildup Factor Coefficients" from *ANSI/ANS 6.4.3*,²¹ while TORT initially used ANSI standard dose factors from the SCALE library.¹⁹ Dose rates were recomputed from TORT scalar fluences using dose factors converted from the ICRP data. Results were compared to GENMASH values and are shown in the Table 8. For the single spatial location, TORT results are up to 40% below the GENMASH results.

2.2.2.7 Computation Time. The TORT calculations referred to above ran on IBM RISC/6000-590 workstations and in general required long computation times (from 700 to 800 minutes for the coarsest mesh and quadrature used to over 1600 minutes for the finest mesh and quadrature used). The total CPU time for the seven TORT 15-photon-group calculations was more than 5400 minutes (3.75 days). About 670 minutes of CPU time were used to perform the ten two-million history, 15-photon-group MASH-MORSE calculations, and about 36 minutes were used for the folding. Thus, the total time expended was more than 6100 minutes (4.24 days). Obviously, the TORT calculation times may be considered excessive for the desired applications. Hence, a simpler, less time-consuming, alternate method was sought. This method is described in Section 3.0.

2.2.3 Test Case 3

A final test case involved the calculation of protection factors at two detector positions within a ten-story concrete building.

2.2.3.1 Source. The source is described in Section 2.2.2.1.

2.2.3.2 Building. The ten-story building, shown in Figure 8, is 3657.6 cm long (X direction), 1828.8 cm wide (Y direction), and 3187.7 cm high (Z direction). Floors and walls are 10.16 cm thick, and there are window openings in the walls. The model also includes a ground region that is 5486.4 cm long, 3657.6 cm wide, and 914.4 cm thick.

2.2.3.3 Calculations. Adjoint MASH-MORSE calculations were performed using both coupled neutron and photon and photon-only DABL69 cross-section libraries. Detectors were located in a hallway corner (X=1840.74cm, Y=30.48cm, Z=1454.7cm) and at the center of the building (X=0.0cm, Y=0.0cm, Z=1454.7cm) for the two MASH-MORSE adjoints. Four of the TORT cases described in Section 2.2.2.3 were rerun (1.0, 3.0, 5.8, and 10.0 h) after minor changes were made in the spatial mesh in order to accommodate the large ten-story building (Section 2.2.3.2) within the revised and extended directional fluence patch boundaries. As with test case 2, directional fluence files were prepared for coupling with the MASH-MORSE adjoints. Fluences and dose rates inside the building were calculated both with and without a plateout source on the roof.

2.2.2.4 Results. Results for the coupled adjoints are shown in Table 9 for a detector located in a hallway corner ($X=840.74\text{cm}$, $Y=30.48\text{cm}$, $Z=1454.7\text{cm}$) and in Table 10 for a detector located at the center of the building ($X=0.0\text{cm}$, $Y=0.0\text{cm}$, $Z=1454.7\text{cm}$). Results for the photon-only adjoints are shown in Table 11 for a detector located in a hallway corner and in Table 12 for a detector located at the center of the building. For these calculations, the adjoint source was nonzero only for photons with energies below 5.0 MeV, although adjoint leakage was scored for all remaining groups of the coupled or photon-only structure. Of more than 180,000 leaking particles for the coupled cases, only about 18,000 (or about 10%) actually contributed to the calculated shielded fluences and doses. For the photon-only cases, about one-third of the leaking particles contributed to the fluences and doses. The results in Tables 9 and 10 show less than 10% variation in the protection factors among the four dose functions for any time step. The highest calculated protection factors are those for time $t=3.0$ h. The tables also show that the plateout source on the roof contributes little in the first two time steps and about 2.5% in the last two time steps. Uncertainties in the spectra for the coupled cases were less than 10% for all except the last three groups ($E < 45$ keV). The uncertainty for group 67 was about 14% while it was about 51% for group 68, which contributes little to the shielded fluences and doses. Group 69 had no contribution. The results in Tables 11 and 12 elicit conclusions similar to those for Tables 9 and 10. However, uncertainties are greater than 10% for the last four groups ($E < 70$ keV) and differences in the protection factors between the coupled and photon-only cases are greater for the centered detector (12 to 20%) than for the off-center detector (up to 4%). Additionally, for the last two time steps, the plateout source on the roof contributes 2.2% to the fluence but less than 1.5% to the dose rate.

3.0 APPROXIMATE METHOD -- COUPLING DIRECTLY WITH PLUME SOURCES

3.1 Description

A method of coupling directly with a plume source (input parameter **idos=3**) was developed in an effort to reduce the overall computation time required to produce the directional fluences to be folded with the MASH-MORSE adjoint leakages. The method is encoded along with all the previous DRC3SRF folding methods in a code called DRC4 for which the input is documented in Appendix A and the file formats are documented in Appendix B. Before the method could be implemented, two additional data files were required. One file is a 3-D quadrature data file with data in a form usable by the code without further processing. The quadratures are used to bin the directional fluences computed by this method. The file is produced by the QUAD3D²² code and is organized such that the number of directions and the quadrature data for a given set are selected based on a four-character name for the quadrature set. For each quadrature set in the file, Table 13 shows the set name, the number of directions, and a brief description. The second file is one that contains as a function of distance, the 1-D angular fluences in various groups resulting from a source (of whatever magnitude) in each source group. The data are treated as if there can be transfers from any one group to any other group, even though in most cases there will be only downscatter. To create the second file, one needs to run **igm** (number of energy groups) ANISN²³ calculations and save the angular fluence files. For the file created to use with the test cases, calculations were run for 18 groups, but only the last 15 were used to create the required file. Also, the air layer thickness was limited to about 5 km due to numerical problems on the IBM RISC 6000 workstations [ANISN is a single-precision arithmetic (32-bit) computer code. A double-precision ANISN might be more appropriate]. Additionally, the point source was normalized to 10^{20} s^{-1} for each group. This high normalization allowed most of the ANISN angular fluences to fall within the range of allowable real numbers on the workstations. The ANISN calculations have to be performed for each air composition desired. The group structure of the ANISN calculations is assumed to be different from the GENMASH and MASH-MORSE group structures. One should use a broad-group structure for the ANISN calculations because disk- and core-storage requirements are reduced and the problem execution time is shortened. Test ANISN calculations were performed for two point source spherical radii (60 cm and 0.62035 cm) and S_{64} and S_{104} quadratures to determine if these parameters had much effect on the total fluences at the ranges of interest. Figure 9 shows a comparison of the group-1 fluence as a function of range for four source combinations. Those results show that outside the radius of the largest sphere, the results for the small and large point sources are not significantly different. Also, the two quadratures produced similar results. Therefore, the 60-cm-radius point source and the S_{64} quadrature used in the ANISN calculations are adequate parameters. The ANISN angular fluence files were processed through the G2GAIR²⁴ code to combine the data into a single file to be used by DRC4. The user specifies the spatial locations (in ascending order) at which the angular fluences will be output (these locations are modified by subtracting from each the parameter **rref** specified by the user). The user also specifies broad angular bins (which may be the same as or a subset of the input ANISN quadrature) into which the output angular fluences will be binned. Input instructions for the QUAD3D and G2GAIR codes are included in

Appendix A and descriptions of the structures of the files output by the codes are in Appendix B. In addition to these two files, the mesh-edged plume source file created by GENMASH is required. A description of that file is also included in Appendix B.

The DRC4 calculational procedure (input parameter **idos=3**) is somewhat like a point kernel calculation, but the spatial attenuation is taken care of by ANISN, and the resulting group-to-group angular fluences replace the buildup factors. While the point kernel method subdivides the source volumes and calculates contributions from each subcell, this method generates a relative mesh around each point at which angular fluences are to be calculated. Sample X-Y plan views of the inner regions of the source integration mesh are shown in Figures 10 and 11. Figure 10 shows the original relatively refined mesh, and Figure 11 shows a coarser mesh. The integration mesh represented by Figure 10 has about six times the total number of cells found in that of Figure 11, and test code calculations showed small differences in the fluences calculated using the two integration meshes. There appears to be little additional contribution from source regions more than 2.5 km away whenever these are not the dominant source regions. Therefore, the mesh in any coordinate direction was limited by the GENMASH source extrema and the maximum allowed distance from the fluence location where contributions are made to the directional fluence. The initial values of the directional fluences in a box^a about the fluence location are calculated as the GENMASH source value at the center of the box times the average fluence one calculates by putting a uniform unit source in the box and calculating the track lengths per unit volume. It was found that sources within the box contribute only a small amount to the total fluence at a given location. Then, for each of the source integration meshes that fall within the established criteria, (1) the interpolation factor for the group $g_{\mathbb{N}}$ to group g angular fluence is determined from the source-to-detector distance and where that distance falls within the G2G AIR output mesh; (2) the 1-D quadrature angles corresponding to each of the 3-D quadrature directions are individually determined; (3) the group $g_{\mathbb{N}}$ to group g angular fluences are determined through interpolation; and (4) a term equal to the product of the source, the interpolated group-to-group angular fluence, and the source point volume or surface leakage factor (area times the cosine with respect to the surface normal) is added to the directional fluence for the appropriate directions and groups. Free-field fluences are calculated by interpolating between integrals of the directional fluences. However, it was noted that the free-field fluences calculated in this manner were lower than those obtained using scalar group-to-group transfers. This may possibly have been due to a lack of quadrature directions falling within the most straight-ahead bin of the ANISN calculation. The original method for which the 1-D quadrature sphere was finely subdivided and contributions were summed into the transformed 3-D quadrature directional bins probably would have given better agreement, but it appeared to be too time-consuming. A remedy for this situation was the normalization of the directional fluence contributions for each source integration mesh to the group scalar fluence contribution based on a scalar group-to-group transfer. Direction \mathbf{m} fluences for ground points, and optionally roof points, are enhanced by the GENMASH ground source value divided by the absolute value of $\mathbf{eta}(\mathbf{m})$, the Z-direction cosine. These

^a50-cm × 50-cm × 50-cm box for a point above the ground (ideally, the point should be more than 25 cm above the ground) and a 50-cm × 50-cm × 25-cm box for a point on the ground.

fluence enhancements may cause the interpolated directional fluences at the side walls to be slightly higher than they should be, since one is interpolating between the higher fluence values on the roof and the unchanged values at points below the roof.

The coordinates of the points [**smesh(3,kpts,ndet)**] at which directional fluences are to be calculated are determined based on several factors. First, an input parameter, **icbrt**, gives the number of points per spatial direction on a box surrounding the MASH-MORSE geometry system (minimum of 2). The total number of points (**kpts**) is **icbrt** cubed (i.e. **icbrt**³). Second the **xo**, **yo**, **zo**, and **to** input arrays give reference locations of the MASH-MORSE system within the GENMASH system and the time at which the fluences are to be calculated (provision is made for interpolating the GENMASH sources to calculate sources for input times that lie within the range of values on the GENMASH source file). The Z extrema of the box for space-time/orientation **jdet** are **zo(jdet)+zmin** and **zo(jdet)+zmax**, where **zo(jdet)** is the input ground surface offset between the GENMASH and MASH-MORSE systems and **zmin** and **zmax** are minimum and maximum Z values of the MASH-MORSE geometry (set **zmin** such that **zo(jdet)+zmin=0.0**). If **icbrt > 2**, then the other Z locations are equally spaced between the Z extrema. The X and Y coordinates are computed such that the MASH-MORSE geometry can be rotated 360 degrees and all parts remain inside the box. This is done by calculating the length of the X-Y diagonal of the MASH-MORSE geometry^b and subtracting that from or adding that to **xo(jdet)** for the X extrema or subtracting from or adding to **yo(jdet)** for the Y extrema. For **icbrt > 2**, other X and Y locations are determined as with Z. Fluences are calculated for **kpts** points for each space-time/orientation **jdet**, and the fluences for any **kdet > jdet** that has the same space-time coordinates as **jdet** are assigned the same fluence values as those computed for space-time/orientation **jdet**. This prevents the recalculation of these quantities for cases having the same space-time coordinates but different orientations. In addition, the DRC4-calculated fluences may be saved on a permanent or temporary file to be used by another case in which the only difference is a change in the detector position in the MASH-MORSE geometry and a corresponding change in the leakage file used (a different file for each detector). A description of the DRC4 directional fluence file is included in Appendix B.

3.2 Testing of the Method

Two test cases for the plume source coupling procedure are cases run with the DRC3SRF **idos=2** option (coupling with TORT boundary directional fluences as described in Section 2.2.2.3). The first test involves the calculation of free-field and shielded fluences and dose rates at ten detector locations in a two-story concrete building with windows and doors for seven time steps as was reported in Section 2.2.2.3. Results for the same time steps and detector positions were obtained by the DRC4 **idos=3** procedure using about 123 minutes of CPU time beyond the 670 minutes required for the ten previously-performed MASH-MORSE calculations. About 80 minutes of the DRC4 time were used to calculate results for the first MASH-MORSE detector position for nine space-time/orientation

^b $\sqrt{(x_{max}&x_{min})^2 + (y_{max}&y_{min})^2}$

combinations. The results from this procedure do not include the effects of ground scatter. A comparison of results obtained using TORT fluences from calculations with and without the ground showed the ground effect to be (1) a 60% increase in the free-field fluence, (2) a 20 to 30% increase in the free-field dose rates, (3) a 20% increase in the fluence protection factor, and (4) a 10% increase in the dose protection factors. The low-energy photon groups contribute more to the free-field fluence than they do to the other three quantities, thus justifying the larger ground effect for the free-field fluence. The **idos=3** procedure of DRC4 is only valid for large dispersed sources having relatively smooth transitions from a given region to adjacent regions. Effects of large localized spikes in the GENMASH source distribution may be missed because of the fixed source-integration mesh.

Results from DRC3SRF and DRC4 for two detector positions and two time steps are compared in Tables 14 and 15, and fluence spectra are compared in Figures 12 and 13. The DRC4 fluences and dose rates are about 50% higher than those calculated by DRC3SRF, but protection factors are in good agreement. As mentioned earlier, the DRC4 results were on the order of the DRC3SRF results before angular fluence contributions were normalized by the scalar fluence contributions of each source integration mesh. However, with the normalization implemented, the ANSI dose rate is on the order of that calculated by GENMASH. One expects agreement with the GENMASH result because both codes ignore ground effects. On the other hand, DRC3SRF results **should be** higher than results calculated by GENMASH or DRC4 with **idos=3**, since ground scatter enhances the fluence levels. While the ground-scatter effect doesn't seem to be very large for the photon-only source, one would expect much larger differences for the coupled neutron-photon case due to the contributions of the secondary photons produced in the ground near the target. However, radiation plumes generally have very little or no neutron emissions.

As mentioned earlier, the DRC4 calculation may use data files in three different group structures: GENMASH, MASH-MORSE, and ANISN group structures. DRC4 calculations were performed to test the effects of the number of rings (**nrad**) in the plume source integration procedure and of the group structure used in the ANISN calculations. Results in Tables 16-21 are for detector position 1 on the first floor of a two-story concrete building. Free-field fluences and dose rates and protection factors are presented for three time steps and six variations on the input data. For Tables 16-18, eight fluence points surround the building (**icbrt=2**) and ANISN air-attenuated angular fluences are for either (1) 43 spatial points and the DABL69 23-photon-group structure or (2) 43 or 82 spatial points and the SCALE 18-photon-group structure. For Tables 19-21, twenty-seven fluence points (**icbrt=3**) define a box that encompasses the building, and other data variations are the same as those used for Tables 16-18. First, the results show that over the first three hours, the fluences, dose rates, and protection factors increase with time. The increase in the protection factors may be due to either a source-spectrum shift with time toward lower energies or a spatial repositioning of the source such that a smaller source fraction has a nearly direct view of the detector through a window. The second observation to note is that increasing **icbrt** from 2 to 3 increases results by a few percent. A third observation to note is that the DABL69 23-photon-group structure gives higher results than the SCALE 18-photon-group structure (A more refined photo energy-group structure than the one available in SCALE might be more appropriate). Finally, using the 18-photon-group air-attenuation data file with 43 spatial points results in higher fluences and dose rates than

those obtained using 82 spatial points, but the protection factors are virtually the same.

The second test problem involves the calculation of dose rates and protection factors for the ten-story building (Figure 8) used in the third test of the rigorous method described in Section 2.2.3 and subsections. Results are shown in Tables 22-27 for centered and off-center detector positions for three variations in the air attenuation file parameters (group structure and the number of air attenuation spatial data points). For the large ten-story building, DRC4 tended to give factors of 1.5 to 2.0 higher fluences than TORT-DRC3SRF for the early times, but the DRC4 results were smaller at later time steps (0.6 to 0.9 times the TORT-DRC3SRF results). DRC4 protection factors were factors of 1.2 to 1.4 times the TORT-DRC3SRF results. The use of ANISN air-attenuated angular fluences calculated with the DABL69 23-photon-group structure (Tables 22 and 23) resulted in slightly higher (< 10%) fluences and protection factors than those obtained using ANISN air-attenuated angular fluences calculated with the SCALE 18-photon-group structure (Tables 24-27). Table 28 compared free-field photon fluences and dose rates calculated with a special code using the SCALE 18-group structure to those calculated with a special code using the DABL69 23-group structure. The codes used the same source integration procedure as DRC4 but calculated results only at the specified points rather than the eight or more locations for which DRC4 calculates fluences before interpolating to get fluences at the points of interest. The fluences for the latter structure were 3% higher and the Straker-Morrison dose rates were about 7% higher. These results are in good agreement. Unlike the results for the first test case above, the protection factors differ by as much as 40% from the DRC3SRF results. Perhaps, an increased number of adjoint histories would improve the results.

3.3 Comparison of DRC4 and GENMASH Free-Field Dose Rates

With regard to the comparison with free-field dose rates computed with GENMASH (Table 8, Section 2.2.2.6), calculations were performed with DRC4 and a test code to see if the source integration procedure would give similar results to GENMASH. The free-field dose rates were on the order of those calculated by GENMASH. However, the detectors were not at the same locations for which the GENMASH dose rates were calculated (i.e. X=1 8.0875 km, Y=55 m, and Z=7.7004 m, and t=1.0 h and 3.0 h). A test program, using the same source integration procedure as DRC4, could calculate results at the precise location, but DRC4 calculates fluences at several locations surrounding the detector location and interpolates on those values to obtain the result at the detector. While DRC4 uses the same source integration method as the test program, the calculated dose rates may be different because the DRC4 result is not calculated at the precise location. Previously, TORT results were obtained by interpolating fluences from the TORT scalar fluence file and folding the fluences with the dose response function. Test program results were obtained for the detector at the above mentioned location, and DRC4 results were obtained for four variations on the input parameters. The results are compared to the GENMASH results in Table 29. As noted in the table, the TORT results are well below the GENMASH results. The test program gave results that are in good agreement with the GENMASH results. The input for the third DRC4 calculation was such that the fluence points were more closely spaced in X and Y than were those in the

first two cases. The fourth DRC4 case was like the third except that the Z spacing of the fluence points was made less. This calculation effectively moves the ground source closer to the detector and may exaggerate the ground source contribution. It is noted that the results for the first DRC4 calculation are slightly higher than the TORT results, but they are still below the GENMASH results by 25%. For this case which used **icbrt=2**, the X and Y extrema are more than 200 m apart, allowing peak fluences in the box to be missed. The second DRC4 case was the same as the first except that **icbrt** was changed to 3. This brought some of the interior fluence points closer to the detector location resulting in smaller errors due to interpolation. The results from this case are in good agreement with GENMASH, being about 2% low at 1.0 h and about 9% low at 3.0 h. The third DRC4 case used the parameters shown in the footnote of Table 18. The X and Y extrema were brought closer to the detector coordinates. The agreement improved slightly from case 2 with the result being about 3% high at 1.0 h and about 5% low at 3.0 h. The results for the fourth DRC4 case are essentially the same as those for DRC4 case 3. Thus, one may improve the DRC4 calculation with the appropriate choice of input parameters, increasing **icbrt** being a choice of last resort. Unfortunately, the fluence must be computed at eight or more locations before the interpolated fluence can be calculated at the detector location of interest. Finally, the test program results are in good agreement with the GENMASH results, being about 7% high at 1.0 h and about 2% low at 3.0 h.

4.0 CONCLUSIONS

An approximate method (DRC4 **idos=3**) for computing fluences, doses, and protection factors in structures from plume sources in air-over-ground environments has been developed and tested. This method and a more rigorous method are described, and calculated results from each are compared with each other and with free-field doses calculated by GENMASH. Compared to the GENMASH point kernel method, the approximate method yields free-field dose rates that are in good agreement. In addition, since time- and energy-dependent directional fluences can be approximated in the vicinity of the structure, one can also estimate shielded fluence spectra and dose rates inside the structure. A great computational time reduction is realized when the approximate method rather than the rigorous method is used, and protection factors appear to be in reasonably good agreement when sufficient adjoint histories are run in the MASH-MORSE calculations.

5.0 REFERENCES

1. G. E. Hansen and H. A. Sandmeier, "Neutron Penetration Factors Obtained by Using Adjoint Transport Calculations," Nucl. Sci. Eng. **22**, 315-320 (July 1965).
2. T. J. Hoffmann, J. C. Robinson, and P. N. Stevens, "The Adjoint Difference Method and Its Application to Deep-Penetration Radiation Transport," Nucl. Sci. Eng. **48**, 179-188 (June 1972).
3. C. O. Slater and J. C. Robinson, "Forward-Adjoint Coupling as a Means of Solving Three-Dimensional Deep-Penetration Transport Problems," Nucl. Sci. Eng. **53**, 332-337 (March 1974).
4. W. A. Rhoades, M. B. Emmett, G. W. Morrison, J. V. Pace, III, and L. M. Petrie, "Vehicle Code System (VCS) User's Manual," Oak Ridge National Laboratory, ORNL/TM-4648 (August 1974).
5. J. O. Johnson, editor, "A User's Manual for MASH 1.0 - A Monte Carlo Adjoint Shielding Code," Oak Ridge National Laboratory, ORNL/TM-11778 (March 1992).
6. C. O. Slater, "DRC2: A Code with Specialized Applications for Coupling Localized Monte Carlo Calculations with Fluences from Two-Dimensional Discrete Ordinates Air-Over-Ground Calculations," Oak Ridge National Laboratory, ORNL/TM-11873 (January 1992).
7. J. O. Johnson, editor, "A User's Manual for MASH v1.5 - A Monte Carlo Adjoint Shielding Code," Oak Ridge National Laboratory, ORNL/TM-11778/R1 (October 1998).
8. J. O. Johnson, editor, "A User's Manual for MASH v2.0 - A Monte Carlo Adjoint Shielding Code," Oak Ridge National Laboratory, ORNL/TM-11778/R2 (1999).
9. Defense Special Weapons Agency, HPAC Version 3.1 Users Guide, Reference Manual Version 7.5 (1996).
10. J. P. Renier, The GENMASH code is an undocumented addition to the HASCAL/SCIPUFF code system.
11. W. A. Rhoades and R. L. Childs, "The TORT Three-Dimensional Discrete Ordinates Neutron/Photon Transport Code," Oak Ridge National Laboratory, ORNL-6268 (November 1987).
12. C. O. Slater, The GENTORT code is documented in Appendix A.

13. W. A. Rhoades and D. B. Simpson, "The TORSET Method for Construction of TORT Boundary Sources from External TORT Fluence Files," Oak Ridge National Laboratory (Draft Document, June 1996), in "DOORS3.1: One-, Two- and Three-Dimensional Discrete Ordinates Neutron/Photon Transport Code System," RSIC Computer Code Collection, CCC-650 (August 1996).
14. C. O. Slater, The PLATEQ code is documented in Appendix A.
15. C. O. Slater, The VIST3DP code is documented in Appendix A.
16. C. O. Slater, The DRC3SRF code is documented in Appendix A.
17. D. T. Ingersoll, R. W. Roussin, C. Y. Fu, and J. E. White, "DABL69: A Broad-Group Neutron/Photon Cross-Section Library for Defense Nuclear Applications," ORNL/TM-10568 (June 1989).
18. The International Committee on Radiological Protection, "ICRP Publication 51," Pergamon Press, New York (1987).
19. American Nuclear Society Standards Committee, "Neutron and Gamma-Ray Cross Sections for Nuclear Radiation Protection Calculations for Nuclear Power Plants," ANSI/ANS-6.1.2, American Nuclear Society, La Grange Park, IL, rev. (1999).
20. C. V. Parks, ed., Scale: A Modular Code System for Performing Standardized Computer Analyses for Licensing Evaluation, NUREG/CR-0200 (ORNL/NUREG/CSD-2/V2/R1), 1983.
21. N. M. Greene, W. E. Ford III, L. M. Petrie, and J. W. Arwood, AMPX: A Modular Code System for Generating Coupled Multigroup Neutron-Gamma Cross-Section Libraries from ENDF/B-IV and/or ENDF/B-V, ORNL/CSD/TM-283 (October 1992).
22. C. O. Slater, The QUAD3D code is documented in Appendix A.
23. W. W. Engle Jr., "ANISN, A One-Dimensional Discrete Ordinates Transport Code With Anisotropic Scattering," Report K-1693 (March, 1967).
24. C. O. Slater, The G2GAIR code is documented in Appendix A.

**Table 1. Atomic Densities ($b^{11} @cm^{11}$) of Elements in Mixtures
Used in the Test Calculations.**

Element	Mixtures					
	Ground ^a	Portland Concrete	Rebar Concrete ^b	Concrete Blocks ^c	Steel	Air ^d
H	4.010! 2 ^e	1.494! 2	1.345! 2	7.673! 3		3.835! 7
C	3.889! 4	3.818! 3	3.793! 3	1.961! 3	3.565! 3	
N	4.896! 5					3.959! 5
O	4.127! 2	4.153! 2	3.738! 2	2.133! 2		1.081! 5
Na	1.470! 4	3.039! 4	2.735! 4	1.561! 4		
Mg	9.403! 5	1.055! 3	9.495! 4	5.418! 4		
Al	1.418! 3	7.372! 4	6.635! 4	3.786! 4		
Si	9.803! 3	6.044! 3	5.440! 3	3.104! 3		
S	3.720! 6					
Cl	3.645! 6					
Ar						2.368! 7
K	2.110! 4	1.217! 4	1.095! 4	6.251! 5		
Ca	2.678! 5	1.159! 2	1.043! 2	5.953! 3		
Cr			3.205! 3		3.205! 3	
Mn	7.418! 6		2.598! 5		2.598! 4	
Fe	3.310! 4	1.974! 4	8.298! 3	1.014! 4	8.120! 2	
Co	2.867! 7					
Ni	2.878! 7					
Cu	5.006! 7					
Sn	7.537! 8					

^a 32% moisture (from ORNL/TM-12685).

^b 0.9 Portland concrete + 0.1 steel by volume.

^c 0.5136 Portland concrete.

^d Air #2 mixture from ORNL/TM-12685.

^e Read as 4.010×10^{12} .

Table 1. (continued)

Element	Mixtures					
	Rebar Concrete 2 ^a	Ground 2	1020 Steel	Air 2	Doors ^b	Windows ^c
H	7.768! 3 ^d	9.75! 3				
C	3.911! 5		7.823! 4		1.299! 4	
N				4.19! 5		
O	4.386! 2	3.48! 2		1.13! 5		8.682! 4
Na	1.336! 3					
Mg	1.484! 6					
Al	2.389! 3	4.88! 3				
Si	1.582! 2	1.16! 2	4.214! 4			4.341! 4
S						
Cl						
Ar				2.51! 7		
K	6.931! 4					
Ca	2.915! 3					
Cr					1.168! 4	
Mn			3.878! 4		9.470! 6	
Fe	4.513! 3		8.401! 2		2.960! 3	
Co						
Ni						
Cu						
Sn						

^a Concrete (composition not shown) + 5% 1020 steel.

^b 0.03645 steel (1.111-cm-thick steel plate smeared over a 30.48-cm thickness).

^c 0.019685 SiO₂ (0.6-cm-thick glass pane smeared over a 30.48-cm-thickness).

^d Read as 7.768×10^{13} .

Table 2. Extent of Structures in the Geometry for TORT/DRC3SRF Test Problem 1.

Coordinate Boundary	System	Ground	Building	Plume ^a
XMIN	! 350000.0	! 350000.0	0.0	! 1000000.0
XMAX	350000.0	350000.0	1737.36	! 300000.0
YMIN	! 350000.0	! 350000.0	0.0	! 5000.0
YMAX	350000.0	350000.0	1463.04	5000.0
ZMIN	! 50.0	! 50.0	0.0	14000.0
ZMAX	50000.0	0.0	640.08	26000.0

^a Plume Volume = $8.4 \times 10^{12} \text{ cm}^3$.

Table 3. Comparison of Dose Rates for Forward-Forward (TORT-TORT) and Forward-Adjoint (TORT-MASH) Couplings.

Position	Source ^a	TORT-TORT (TT)	TORT-MASH (TM)	f.s.d. ^b	TM/TT
1	A	1.79! 19 ^c	2.09! 19	0.031	1.17
	B	1.79! 19	2.09! 19	0.031	1.17
2	A	5.87! 20	6.31! 20	0.035	1.07
	B	5.88! 20	6.30! 20	0.035	1.07
3	A	3.50! 22	6.34! 22	0.25	1.81
	B	3.43! 22	5.92! 22	0.27	1.72
4	A	1.71! 21	2.35! 21	0.25	1.37
	B	1.72! 21	2.31! 21	0.25	1.34
5	A	3.92! 22	3.98! 22	0.29	1.02
	B	3.80! 22	3.62! 22	0.32	0.95
6	A	2.11! 19	2.40! 19	0.026	1.13
	B	2.10! 19	2.38! 19	0.026	1.13
7	A	7.77! 20	8.72! 20	0.049	1.12
	B	7.72! 20	8.62! 20	0.050	1.12
8	A	4.48! 21	4.59! 21	0.14	1.03
	B	3.64! 21	3.67! 21	0.17	1.01
9	A	9.25! 21	8.93! 21	0.18	0.97
	B	8.30! 21	7.29! 21	0.22	0.88
10	A	6.08! 21	7.33! 21	0.11	1.21
	B	5.27! 21	6.17! 21	0.13	1.17

^a (A): Plume source plus uniform isotropic source on roof. (B): Plume source only.

^b Fractional standard deviation of the TM result.

^c Read as 1.79×10^{19} .

Table 4. Energy Boundaries for the Photon Group Structures Used in the Calculations.

Group	Group Energy Boundaries (eV)		
	MASH-MORSE ^a	GENMASH ^b	TORT ^c
1	1.40+7 ^d	1.40+7	1.00+7
2	1.00+7	1.00+7	8.00+6
3	8.00+6	8.00+6	6.50+6
4	7.50+6	7.00+6	5.00+6
5	7.00+6	6.00+6	4.00+6
6	6.00+6	5.00+6	3.00+6
7	5.00+6	4.00+6	2.50+6
8	4.00+6	3.00+6	2.00+6
9	3.00+6	2.50+6	1.66+6
10	2.50+6	2.00+6	1.33+6
11	2.00+6	1.50+6	1.00+6
12	1.50+6	1.00+6	8.00+5
13	1.00+6	7.00+5	6.00+5
14	7.00+5	4.50+5	4.00+5
15	6.00+5	3.00+5	3.00+5
16	5.10+5	1.50+5	2.00+5
17	4.00+5	6.00+4	1.00+5
18	3.00+5	3.00+4	5.00+4
19	1.50+5	1.00+4 ^e	1.00+4 ^e
20	1.00+5		
21	7.00+4		
22	4.50+4		
23	2.00+4		
24	1.00+4 ^e		

^a DABL69 46n/23g group structure.¹⁷

^b AMPX¹⁸ Standard 18-group photon structure.

^c Structure for SCALE¹⁹ 18-group photon library. ^d Read as 1.4×10^7 .

^e Lower energy boundary for the group structure.

Table 5. ANSI Standard Photon Dose Rates (rem/h) at Detector Locations Inside a Two-Story Concrete Building.

Detector	Time (h)						
	1.0	2.0	3.0	4.4	5.8	7.2	10.0
1	5.09+0 ^a	7.11+0	8.07+0	1.56! 2	1.47! 2	1.40! 2	1.30! 2
2	1.51+0	2.03+0	2.25+0	4.30! 3	3.98! 3	3.76! 3	3.46! 3
3	4.31! 1	5.77! 1	6.37! 1	1.11! 3	1.03! 3	9.72! 4	8.95! 4
4	1.69+0	2.29+0	2.55+0	5.31! 3	4.93! 3	4.66! 3	4.31! 3
5	8.03! 1	1.09+0	1.21+0	2.03! 3	1.88! 3	1.78! 3	1.65! 3
6	6.43+0	8.92+0	1.01+1	1.62! 2	1.51! 2	1.44! 2	1.34! 2
7	2.47+0	3.33+0	3.70+0	5.81! 3	5.37! 3	5.07! 3	4.67! 3
8	1.32+0	1.77+0	1.96+0	2.89! 3	2.67! 3	2.52! 3	2.32! 3
9	2.88+0	3.90+0	4.34+0	6.94! 3	6.42! 3	6.08! 3	5.60! 3
10	1.95+0	2.64+0	2.94+0	4.21! 3	3.89! 3	3.68! 3	3.40! 3

^a Read as 5.09×10^0 .

Table 6. ANSI Standard Free-Field Photon Dose Rates (rem/h) at Detector Locations Inside a Two-Story Concrete Building.

Detector	Time (h)						
	1.0	2.0	3.0	4.4	5.8	7.2	10.0
1	3.36+1 ^a	4.80+1	5.55+1	7.86! 2	7.45! 2	7.17! 2	6.74! 2
2	3.33+1	4.77+1	5.51+1	7.41! 2	7.03! 2	6.76! 2	6.36! 2
3	3.22+1	4.60+1	5.30+1	5.09! 2	4.83! 2	4.65! 2	4.38! 2
4	3.35+1	4.79+1	5.53+1	7.54! 2	7.16! 2	6.88! 2	6.48! 2
5	3.23+1	4.61+1	5.32+1	5.12! 2	4.86! 2	4.67! 2	4.40! 2
6	3.58+1	5.13+1	5.94+1	1.18! 1	1.12! 1	1.07! 1	1.01! 1
7	3.56+1	5.10+1	5.90+1	1.18! 1	1.12! 1	1.07! 1	1.00! 1
8	3.45+1	4.94+1	5.72+1	1.20! 1	1.14! 1	1.08! 1	1.02! 1
9	3.58+1	5.13+1	5.94+1	1.19! 1	1.13! 1	1.08! 1	1.02! 1
10	3.46+1	4.96+1	5.74+1	1.20! 1	1.13! 1	1.09! 1	1.02! 1

^a Read as 3.36×10^1 .

Table 7. ANSI Standard Photon Dose-Rate Protection Factors at Detector Locations Inside a Two-Story Concrete Building.

Detector	Time (h)						
	1.0	2.0	3.0	4.4	5.8	7.2	10.0
1	6.59+0 ^a	6.76+0	6.87+0	5.03+0	5.09+0	5.13+0	5.17+0
2	2.21+1	2.35+1	2.45+1	1.72+1	1.77+1	1.80+1	1.84+1
3	7.47+1	7.96+1	8.33+1	4.57+1	4.70+1	4.79+1	4.89+1
4	1.98+1	2.09+1	2.17+1	1.42+1	1.45+1	1.48+1	1.50+1
5	4.02+1	4.24+1	4.40+1	2.52+1	2.58+1	2.62+1	2.67+1
6	5.57+0	5.76+0	5.89+0	7.31+0	7.40+0	7.45+0	7.52+0
7	1.44+1	1.53+1	1.60+1	2.03+1	2.08+1	2.11+1	2.15+1
8	2.62+1	2.79+1	2.92+1	4.15+1	4.25+1	4.57+1	4.41+1
9	1.24+1	1.32+1	1.37+1	1.72+1	1.76+1	1.78+1	1.82+1
10	1.77+1	1.88+1	1.95+1	2.85+1	2.91+1	2.96+1	3.01+1

^a Read as 6.59×10^0 .

**Table 8. Comparisons of TORT and GENMASH Free-Field Dose Rates
at X=-8.0875 km, Y=55 m, and Z=7.7004 m.**

Time After Accident (h)	Gamma-Ray Dose Rate (rem/h)		$\left(\frac{TORT}{GENMASH} \& 1.0 \right) \times 100$
	GENMASH	TORT	
1.0	38.57	24.73	-35.9
3.0	67.51	40.26	-40.36

Table 9. TORT/DRC3SRF Free-Field Fluence and Dose Rate and Protection Factors at a Corner Detector Position in a Large, Thin-Walled Building for a Plume Photon Source at Several Time Intervals (Coupled neutron and photon adjoint).

Quantity	Time (h)			
	1.0	3.0	5.8	10.0
Free-Field Values				
Fluence ^a	4.649+7 ^b	8.262+7	8.833+4	8.098+4
Dose 1 ^c	2.475+1	4.015+1	4.531! 2	4.035! 2
Dose 2 ^c	2.931+1	4.740+1	5.352! 2	4.758! 2
Dose 3 ^c	3.884+1	6.420+1	7.164! 2	6.413! 2
Dose 4 ^c	3.351+1	5.565+1	6.207! 2	5.570! 2
Protection Factors For Ground, Plume, and Roof Sources				
Fluence ^a	36.95	40.97	33.29	34.46
Dose 1 ^c	30.75	33.26	28.34	29.16
Dose 2 ^c	31.70	34.48	29.41	30.32
Dose 3 ^c	32.97	36.12	30.46	31.45
Dose 4 ^c	32.36	35.30	29.72	30.65
Protection Factors for Ground and Plume Sources				
Fluence ^a	36.96	40.99	34.19	35.38
Dose 1 ^c	30.75	33.26	29.03	29.88
Dose 2 ^c	31.70	34.49	30.11	31.05
Dose 3 ^c	32.97	36.13	31.19	32.22
Dose 4 ^c	32.36	35.31	30.46	31.42

^a cm¹² @s¹¹.

^b Read as 4.649 × 10⁷.

^c Doses 1-4 are respectively Straker-Morrison, Henderson, Claiborne-Trubey, and ANSI standard with units of rem/h.¹⁹

Table 10. TORT/DRC3SRF Free-Field Fluence and Dose Rate and Protection Factors at a Center Detector Position in a Large, Thin-Walled Building for a Plume Photon Source at Several Time Intervals (Coupled neutron and photon adjoint).

Quantity	Time (h)			
	1.0	3.0	5.8	10.0
Free-Field Values				
Fluence ^a	4.589+7 ^b	8.153+7	8.688+4	7.965+4
Dose 1 ^c	2.432+1	3.944+1	4.448! 2	3.962! 2
Dose 2 ^c	2.878+1	4.654+1	5.253! 2	4.669! 2
Dose 3 ^c	3.818+1	6.310+1	7.034! 2	6.297! 2
Dose 4 ^c	3.295+1	5.472+1	6.095! 2	5.468! 2
Protection Factors For Ground, Plume, and Roof Sources				
Fluence ^a	36.18	40.23	32.30	33.42
Dose 1 ^c	29.95	32.46	27.93	28.72
Dose 2 ^c	30.93	33.72	29.08	29.97
Dose 3 ^c	32.20	35.36	30.03	31.00
Dose 4 ^c	31.55	34.50	29.22	30.13
Protection Factors for Ground and Plume Sources				
Fluence ^a	36.19	40.24	33.19	34.34
Dose 1 ^c	29.95	32.46	28.54	29.36
Dose 2 ^c	30.93	33.73	29.70	30.61
Dose 3 ^c	32.20	35.37	30.70	31.70
Dose 4 ^c	31.55	34.50	29.89	30.83

^a cm¹² @s¹¹.

^b Read as 4.589 × 10⁷.

^c Doses 1-4 are respectively Straker-Morrison, Henderson, Claiborne-Trubey, and ANSI standard with units of rem/h.¹⁹

Table 11. TORT/DRC3SRF Free-Field Fluence and Dose Rate and Protection Factors at a Corner Detector Position in a Large, Thin-Walled Building for a Plume Photon Source at Several Time Intervals (Photon only adjoint).

Quantity	Time (h)			
	1.0	3.0	5.8	10.0
Free-Field Values				
Fluence ^a	4.649+7 ^b	8.262+7	8.833+4	8.098+4
Dose 1 ^c	2.475+1	4.015+1	4.531! 2	4.035! 2
Dose 2 ^c	2.931+1	4.740+1	5.352! 2	4.758! 2
Dose 3 ^c	3.884+1	6.420+1	7.164! 2	6.413! 2
Dose 4 ^c	3.351+1	5.565+1	6.207! 2	5.570! 2
Protection Factors For Ground, Plume, and Roof Sources				
Fluence ^a	36.27	40.24	32.23	33.33
Dose 1 ^c	29.74	32.16	27.96	28.72
Dose 2 ^c	30.65	33.32	29.26	30.11
Dose 3 ^c	31.94	35.00	30.17	31.10
Dose 4 ^c	31.34	34.20	29.19	30.06
Protection Factors for Ground and Plume Sources				
Fluence ^a	36.27	40.26	33.00	34.13
Dose 1 ^c	29.74	32.16	28.63	29.41
Dose 2 ^c	30.65	33.33	29.96	30.84
Dose 3 ^c	31.95	35.01	30.89	31.85
Dose 4 ^c	31.35	34.21	29.89	30.79

^a cm¹² @s¹¹.

^b Read as 4.649 × 10⁷.

^c Doses 1-4 are respectively Straker-Morrison, Henderson, Claiborne-Trubey, and ANSI standard with units of rem/h.¹⁹

Table 12. Free-Field Fluence and Dose Rate and Protection Factors at a Center Detector Position in a Large, Thin-Walled Building for a Plume Photon Source at Several Time Intervals (Photon only adjoint).

Quantity	Time (h)			
	1.0	3.0	5.8	10.0
Free-Field Values				
Fluence ^a	4.589+7 ^b	8.153+7	8.688+4	7.965+4
Dose 1 ^c	2.432+1	3.944+1	4.448! 2	3.962! 2
Dose 2 ^c	2.878+1	4.654+1	5.253! 2	4.669! 2
Dose 3 ^c	3.818+1	6.310+1	7.034! 2	6.297! 2
Dose 4 ^c	3.295+1	5.472+1	6.095! 2	5.468! 2
Protection Factors For Ground, Plume, and Roof Sources				
Fluence ^a	41.52	46.11	38.68	40.07
Dose 1 ^c	33.97	36.81	33.40	34.46
Dose 2 ^c	34.96	38.10	34.68	35.85
Dose 3 ^c	36.48	40.05	35.83	37.10
Dose 4 ^c	35.85	39.20	34.98	36.16
Protection Factors for Ground and Plume Sources				
Fluence ^a	41.53	46.12	39.52	40.95
Dose 1 ^c	33.98	36.82	33.85	34.92
Dose 2 ^c	34.96	38.10	35.09	36.28
Dose 3 ^c	36.48	40.05	36.32	37.60
Dose 4 ^c	35.85	39.20	35.50	36.70

^a cm¹² @s¹¹.

^b Read as 4.589 × 10⁷.

^c Doses 1-4 are respectively Straker-Morrison, Henderson, Claiborne-Trubey, and ANSI standard with units of rem/h.¹⁹

Table 13. Descriptions of the 3-D Quadrature Sets on the File Created by QUAD3D.

Set Number	Set Name	Number of Directions	Description
1	s8	96	symmetric S_8
2	s10	140	symmetric S_{10}
3	s12	192	symmetric S_{12}
4	s14	252	symmetric S_{14}
5	s16	320	symmetric S_{16}
6	d200	200	downward biased set (130 down)
7	u200	200	upward biased set (130 up)
8	d332	332	downward biased set (262 down)
9	u332	332	upward biased set (262 up)
10	d420	420	downward biased set (306 down)
11	u420	420	upward biased set (306 up)
12	d630	630	downward biased set (560 down)
13	u630	630	upward biased set (560 up)

Table 14. Free-Field Data and Protection Factors for a Detector at Position 1 in a Two-Story Building. The DRC4 calculation used a 22-angle 1-D quadrature and an S_8 3-D quadrature to bin the 3-D fluences at eight fluence points surrounding the building for each time step (calculation time ~23 min. for two time steps).

Time Step	Quantity ^a	DRC3SRF	DRC4	DRC3SRF/DRC4
Free-Field Data				
1	Fluence	4.754+7 ^b	7.205+7	0.66
	Dose 1	25.16	40.28	0.62
	Dose 2	29.24	47.62	0.61
	Dose 3	38.61	62.17	0.62
	Dose 4	33.57	53.38	0.63
2	Fluence	7.110+7	1.082+8	0.66
	Dose 1	35.47	56.85	0.62
	Dose 2	41.08	67.07	0.61
	Dose 3	55.01	88.80	0.62
	Dose 4	48.01	76.50	0.63
Protection Factors				
1	Fluence	7.86	8.11	0.97
	Dose 1	6.26	6.66	0.94
	Dose 2	6.33	6.82	0.93
	Dose 3	6.63	7.10	0.93
	Dose 4	6.59	6.99	0.94
2	Fluence	8.05	8.34	0.97
	Dose 1	6.40	6.81	0.94
	Dose 2	6.49	7.01	0.93
	Dose 3	6.82	7.31	0.93
	Dose 4	6.76	7.19	0.94

^a Doses 1-4 are respectively Straker-Morrison, Henderson, Claiborne-Trubey, and ANSI standard with

units of rem/h.¹⁹ The fluence has units of $\text{cm}^2 \text{s}^{-1}$.
^b Read as 4.754×10^7 .

Table 15. Free-Field Data and Protection Factors for a Detector at Position 2 in a Two-Story Building. The DRC4 calculation used a 22-angle 1-D quadrature and an S_8 3-D quadrature to bin the 3-D fluences at eight fluence points surrounding the building for each time step (calculation time 1.2 min. for two time steps because of time savings from the Table 1 calculations).

Time Step	Quantity ^a	DRC3SRF	DRC4	DRC3SRF/DRC4
Free-Field Data				
1	Fluence	4.726+7 ^b	7.205+7	0.66
	Dose 1	24.99	40.28	0.62
	Dose 2	29.02	47.62	0.61
	Dose 3	38.33	62.17	0.62
	Dose 4	33.34	53.38	0.62
2	Fluence	7.068+7	1.082+8	0.65
	Dose 1	35.23	56.85	0.62
	Dose 2	40.77	67.07	0.61
	Dose 3	54.60	88.80	0.61
	Dose 4	47.67	76.50	0.62
Protection Factors				
1	Fluence	30.28	30.98	0.98
	Dose 1	20.57	21.81	0.94
	Dose 2	20.80	22.39	0.93
	Dose 3	22.35	23.86	0.94
	Dose 4	22.13	23.39	0.95
2	Fluence	32.55	33.49	0.97
	Dose 1	21.67	23.03	0.94
	Dose 2	21.97	23.72	0.93
	Dose 3	23.77	25.45	0.93
	Dose 4	23.48	24.88	0.94

^a Doses 1-4 are respectively Straker-Morrison, Henderson, Claiborne-Trubey, and ANSI standard with

units of rem/h.¹⁹ The fluence has units of $\text{cm}^2 \text{s}^{-1}$.
^b Read as 4.726×10^7 .

Table 16. Free-field fluences ($\text{cm}^{12} \text{ @s}^{11}$) and dose rates (rem/h) for detector 1 in a two-story concrete building (icbrt=2^a; nrad=43^a; DABL69 23-group photon structure; time=38.8 min).

Quantity	Time (h)		
	1.0	2.0	3.0
Fluences and Dose Rates			
Fluence	7.701+7 ^b	1.157+8	1.381+8
Dose 1 ^c	43.90	62.14	71.30
Dose 2 ^c	56.19	80.05	92.24
Dose 3 ^c	73.78	106.5	123.7
Dose 4 ^c	60.97	87.93	102.2
Dose 5 ^c	42.16	59.70	68.54
Protection Factors for Fluences and Dose Rates			
Fluence	8.66	8.94	9.12
Dose 1 ^c	7.13	7.32	7.45
Dose 2 ^c	7.89	8.20	8.42
Dose 3 ^c	8.26	8.61	8.86
Dose 4 ^c	7.84	8.12	8.31
Dose 5 ^c	6.93	7.08	7.19

^a **icbrt** is the number of fluence points per side of a box surrounding the region of interest and **nrad** is the number of radial distances at which ANISN air-attenuated angular fluences are given).

^b Read as 7.701×10^7 .

^c Doses 1-5 are respectively Straker-Morrison,¹⁹ Henderson,¹⁹ Claiborne-Trubey,¹⁹ ANSI standard,¹⁹ and the AP photon dose rate in a phantom.²⁰

Table 17. Free-field fluences ($\text{cm}^{12} \text{ @s}^{11}$) and dose rates (rem/h) for detector 1 in a two-story concrete building (icbrt=2^a; nrad=82^a; SCALE 18-group photon structure; time=34.2 min).

Quantity	Time (h)		
	1.0	2.0	3.0
Fluences and Dose Rates			
Fluence	7.125+7 ^b	1.070+8	1.277+8
Dose 1 ^c	39.80	56.18	64.35
Dose 2 ^c	47.05	66.27	75.79
Dose 3 ^c	61.44	87.76	101.3
Dose 4 ^c	52.75	75.61	87.50
Dose 5 ^c	39.45	55.92	64.23
Protection Factors for Fluences and Dose Rates			
Fluence	8.13	8.36	8.50
Dose 1 ^c	6.68	6.83	6.93
Dose 2 ^c	6.84	7.03	7.16
Dose 3 ^c	7.11	7.33	7.48
Dose 4 ^c	7.01	7.20	7.34
Dose 5 ^c	6.69	6.83	6.93

^a **icbrt** is the number of fluence points per side of a box surrounding the region of interest and **nrad** is the number of radial distances at which ANISN air-attenuated angular fluences are given).

^b Read as 7.125×10^7 .

^c Doses 1-5 are respectively Straker-Morrison,¹⁹ Henderson,¹⁹ Claiborne-Trubey,¹⁹ ANSI standard,¹⁹ and the AP photon dose rate in a phantom.²⁰

Table 18. Free-field fluences ($\text{cm}^{12} \text{ @s}^{11}$) and dose rates (rem/h) for detector 1 in a two-story concrete building (icbrt=2^a; nrad=43^a; SCALE 18-group photon structure; time=34.1 min).

Quantity	Time (h)		
	1.0	2.0	3.0
Fluences and Dose Rates			
Fluence	7.318+7 ^b	1.099+8	1.310+8
Dose 1 ^c	40.57	57.26	65.58
Dose 2 ^c	47.93	67.49	77.18
Dose 3 ^c	62.68	89.51	103.3
Dose 4 ^c	53.84	77.14	89.27
Dose 5 ^c	40.24	57.03	65.60
Protection Factors for Fluences and Dose Rates			
Fluence	8.13	8.36	8.50
Dose 1 ^c	6.65	6.80	6.91
Dose 2 ^c	6.81	6.99	7.13
Dose 3 ^c	7.08	7.30	7.45
Dose 4 ^c	6.98	7.18	7.31
Dose 5 ^c	6.66	6.81	6.91

^a **icbrt** is the number of fluence points per side of a box surrounding the region of interest and **nrad** is the number of radial distances at which ANISN air-attenuated angular fluences are given).

^b Read as 7.318×10^7 .

^c Doses 1-5 are respectively Straker-Morrison,¹⁹ Henderson,¹⁹ Claiborne-Trubey,¹⁹ ANSI standard,¹⁹ and the AP photon dose rate in a phantom.²⁰

Table 19. Free-field fluences ($\text{cm}^{12} \text{ @s}^{11}$) and dose rates (rem/h) for detector 1 in a two-story concrete building (icbrt=3^a; nrad=43^a; DABL69 23-group photon structure; time=132.5 min).

Quantity	Time (h)		
	1.0	2.0	3.0
Fluences and Dose Rates			
Fluence	7.869+7 ^b	1.183+8	1.411+8
Dose 1 ^c	45.20	63.95	73.36
Dose 2 ^c	57.85	82.39	94.90
Dose 3 ^c	75.85	109.4	127.1
Dose 4 ^c	62.66	90.36	105.0
Dose 5 ^c	43.38	61.42	70.49
Protection Factors for Fluences and Dose Rates			
Fluence	8.54	8.82	9.00
Dose 1 ^c	7.03	7.21	7.35
Dose 2 ^c	7.77	8.08	8.30
Dose 3 ^c	8.14	8.49	8.73
Dose 4 ^c	7.73	8.00	8.19
Dose 5 ^c	6.83	6.98	7.09

^a **icbrt** is the number of fluence points per side of a box surrounding the region of interest and **nrad** is the number of radial distances at which ANISN air-attenuated angular fluences are given).

^b Read as 7.869×10^7 .

^c Doses 1-5 are respectively Straker-Morrison,¹⁹ Henderson,¹⁹ Claiborne-Trubey,¹⁹ ANSI standard,¹⁹ and the AP photon dose rate in a phantom.²⁰

Table 20. Free-field fluences ($\text{cm}^{12} \text{ @s}^{11}$) and dose rates (rem/h) for detector 1 in a two-story concrete building (icbrt=3^a; nrad=82^a; scale 18-group photon structure; time=116.2 min).

Quantity	Time (h)		
	1.0	2.0	3.0
Fluences and Dose Rates			
Fluence	7.288+7 ^b	1.095+8	1.306+8
Dose 1 ^c	41.05	57.93	66.34
Dose 2 ^c	48.63	68.49	78.31
Dose 3 ^c	63.41	90.56	104.5
Dose 4 ^c	54.38	77.92	90.17
Dose 5 ^c	40.64	57.59	66.13
Protection Factors for Fluences and Dose Rates			
Fluence	8.02	8.25	8.39
Dose 1 ^c	6.59	6.74	6.84
Dose 2 ^c	6.76	6.95	7.08
Dose 3 ^c	7.03	7.24	7.40
Dose 4 ^c	6.92	7.11	7.25
Dose 5 ^c	6.59	6.74	6.84

^a **icbrt** is the number of fluence points per side of a box surrounding the region of interest and **nrad** is the number of radial distances at which ANISN air-attenuated angular fluences are given).

^b Read as 7.288×10^7 .

^c Doses 1-5 are respectively Straker-Morrison,¹⁹ Henderson,¹⁹ Claiborne-Trubey,¹⁹ ANSI standard,¹⁹ and the AP photon dose rate in a phantom.²⁰

Table 21. Free-field fluences ($\text{cm}^{12} \text{ @s}^{11}$) and dose rates (rem/h) for detector 1 in a two-story concrete building (icbrt=3^a; nrad=43^a; scale 18-group photon structure; time=116.0 min).

Quantity	Time (h)		
	1.0	2.0	3.0
Fluences and Dose Rates			
Fluence	7.478+7 ^b	1.123+8	1.339+8
Dose 1 ^c	41.81	58.99	67.55
Dose 2 ^c	49.50	69.70	79.69
Dose 3 ^c	64.63	92.29	106.5
Dose 4 ^c	55.45	79.44	91.92
Dose 5 ^c	41.42	56.68	67.38
Protection Factors for Fluences and Dose Rates			
Fluence	8.02	8.25	8.40
Dose 1 ^c	6.56	6.71	6.82
Dose 2 ^c	6.73	6.92	7.05
Dose 3 ^c	7.00	7.22	7.37
Dose 4 ^c	6.90	7.09	7.23
Dose 5 ^c	6.57	6.72	6.82

^a **icbrt** is the number of fluence points per side of a box surrounding the region of interest and **nrad** is the number of radial distances at which ANISN air-attenuated angular fluences are given).

^b Read as 7.478×10^7 .

^c Doses 1-5 are respectively Straker-Morrison,¹⁹ Henderson,¹⁹ Claiborne-Trubey,¹⁹ ANSI standard,¹⁹ and the AP photon dose rate in a phantom.²⁰

Table 22. Comparison of TORT-DRC3SRF and DRC4 Fluences and Protection Factors for an Off-Center Detector in the Ten-Story NGIC Building D (includes roof source contribution; air attenuation by a 23-group photon library; attenuation data given for 43 distances).

Time (h)	TORT-DRC3SRF	DRC4	DRC4/TORT-DRC3SRF
Free-Field Fluences			
1.0	4.649+7 ^a	8.981+7	1.93
3.0	8.262+7	1.612+8	1.95
5.8	8.833+4	7.590+4	0.86
10.0	8.098+4	7.004+4	0.86
Shielded Fluences			
1.0	1.282+6	1.890+6	1.47
3.0	2.053+6	3.005+6	1.46
5.8	2.741+3	1.643+3	0.60
10.0	2.430+3	1.458+3	0.60
Protection Factors			
1.0	36.27	47.51	1.31
3.0	40.24	53.63	1.33
5.8	32.23	46.19	1.43
10.0	33.33	48.04	1.44

^a Read as 4.649×10^7 .

Table 23. Comparison of TORT-DRC3SRF and DRC4 Fluences and Protection Factors for a Centered Detector in the Ten-Story NGIC Building D (includes roof source contribution; air attenuation by a 23-group photon library; attenuation data given for 43 distances).

Time (h)	TORT-DRC3SRF	DRC4	DRC4/TORT-DRC3SRF
Free-Field Fluences			
1.0	4.589+7 ^a	8.995+7	1.96
3.0	8.153+7	1.614+8	1.98
5.8	8.688+4	7.605+4	0.88
10.0	7.965+4	7.018+4	0.88
Shielded Fluences			
1.0	1.105+6	1.686+6	1.53
3.0	1.768+6	2.675+6	1.51
5.8	2.246+3	1.424+3	0.63
10.0	1.988+3	1.260+3	0.63
Protection Factors			
1.0	41.52	53.36	1.29
3.0	46.11	60.34	1.31
5.8	38.68	53.40	1.38
10.0	40.07	55.69	1.39

^a Read as 4.589×10^7 .

Table 24. Comparison of TORT-DRC3SRF and DRC4 Fluences and Protection Factors for an Off-Center Detector in the Ten-Story NGIC Building D (includes roof source contribution; air attenuation by an 18-group photon library; attenuation data given for 82 distances).

Time (h)	TORT-DRC3SRF	DRC4	DRC4/TORT-DRC3SRF
Free-Field Fluences			
1.0	4.649+7 ^a	8.338+7	1.79
3.0	8.262+7	1.495+8	1.81
5.8	8.833+4	7.220+4	0.82
10.0	8.098+4	6.661+4	0.82
Shielded Fluences			
1.0	1.282+6	1.841+6	1.44
3.0	2.053+6	2.955+6	1.44
5.8	2.741+3	1.614+3	0.59
10.0	2.430+3	1.435+3	0.59
Protection Factors			
1.0	36.27	45.28	1.25
3.0	40.24	50.60	1.26
5.8	32.23	44.73	1.39
10.0	33.33	46.42	1.39

^a Read as 4.649×10^7 .

Table 25. Comparison of TORT-DRC3SRF and DRC4 Fluences and Protection Factors for a Centered Detector in the Ten-Story NGIC Building D (includes roof source contribution; air attenuation by an 18-group photon library; attenuation data given for 82 distances).

Time (h)	TORT-DRC3SRF	DRC4	DRC4/TORT-DRC3SRF
Free-Field Fluences			
1.0	4.589+7 ^a	8.352+7	1.82
3.0	8.153+7	1.498+8	1.84
5.8	8.688+4	7.287+4	0.84
10.0	7.965+4	6.723+4	0.84
Shielded Fluences			
1.0	1.105+6	1.634+6	1.48
3.0	1.768+6	2.619+6	1.48
5.8	2.246+3	1.391+3	0.62
10.0	1.988+3	1.234+3	0.62
Protection Factors			
1.0	41.52	51.11	1.23
3.0	46.11	57.18	1.24
5.8	38.68	52.38	1.35
10.0	40.07	54.49	1.36

^a Read as 4.589×10^7 .

Table 26. Comparison of TORT-DRC3SRF and DRC4 Fluences and Protection Factors for an Off-Center Detector in the Ten-Story NGIC Building D (includes roof source contribution; air attenuation by an 18-group photon library; attenuation data given for 43 distances).

Time (h)	TORT-DRC3SRF	DRC4	DRC4/TORT-DRC3SRF
Free-Field Fluences			
1.0	4.649+7 ^a	8.528+7	1.83
3.0	8.262+7	1.528+8	1.85
5.8	8.833+4	7.241+4	0.82
10.0	8.098+4	6.680+4	0.82
Shielded Fluences			
1.0	1.282+6	1.875+6	1.46
3.0	2.053+6	3.008+6	1.47
5.8	2.741+3	1.619+3	0.59
10.0	2.430+3	1.440+3	0.59
Protection Factors			
1.0	36.27	45.48	1.25
3.0	40.24	50.79	1.26
5.8	32.23	44.72	1.39
10.0	33.33	46.40	1.39

^a Read as 4.649×10^7 .

Table 27. Comparison of TORT-DRC3SRF and DRC4 Fluences and Protection Factors for a Centered Detector in the Ten-Story NGIC Building D (includes roof source contribution; air attenuation by an 18-group photon library; attenuation data given for 43 distances).

Time (h)	TORT-DRC3SRF	DRC4	DRC4/TORT-DRC3SRF
Free-Field Fluences			
1.0	4.589+7 ^a	8.541+7	1.86
3.0	8.153+7	1.530+8	1.88
5.8	8.688+4	7.308+4	0.84
10.0	7.965+4	6.742+4	0.85
Shielded Fluences			
1.0	1.105+6	1.663+6	1.50
3.0	1.768+6	2.665+6	1.51
5.8	2.246+3	1.396+3	0.62
10.0	1.988+3	1.238+3	0.62
Protection Factors			
1.0	41.52	51.35	1.24
3.0	46.11	57.43	1.25
5.8	38.68	52.36	1.35
10.0	40.07	54.48	1.36

^a Read as 4.589×10^7 .

Table 28. Comparison of fluences and dose rates calculated by special codes using GENMASH sources, the DRC4 source-integration procedure, and ANISN air-attenuated angular fluences in two group structures.

Time (h)	Detector 1 ^a			Detector 2 ^a		
	Grp.-A ^b	Grp.-B ^b	Grp.-B/Grp.-A	Grp.-A ^b	Grp.-B ^b	Grp.-B/Grp.-A
Fluence						
1.0	8.732+7 ^c	8.967+7	1.03	8.742+7	8.978+7	1.03
2.0	1.302+8	1.337+8	1.03	1.303+8	1.338+8	1.03
3.0	1.543+8	1.548+8	1.03	1.545+8	1.586+8	1.03
Straker-Morrison Dose Rate (rem/h)						
1.0	45.60	48.82	1.07	45.66	48.89	1.07
2.0	64.08	68.76	1.07	64.16	68.85	1.07
3.0	73.04	78.51	1.07	73.13	78.61	1.07

^a Detector 1 is off centerline and is located at the coordinates (-8.0084e5, 30.48, 1454.7) relative to the GENMASH source mesh. The on-centerline detector 2 is located at the coordinates (-8.0e5, 0.0, 1454.7). The coordinate unit is cm.

^b Grp.-A is the bottom 15 groups of the SCALE 18-group photon structure and Grp.-B is the bottom 16 groups of the DABL69 23-group photon structure.

^c Read as 8.732×10^7 .

Table 29. Comparison of GENMASH dose rates with TORT, DRC4, and Test Program dose rates.

Method	Time (h)			
	1.0		3.0	
	Dose Rate (rem/h)	% Diff.	Dose Rate (rem/h)	% Diff.
GENMASH	38.57	0.0	67.51	0.0
TORT	24.73	! 35.9	40.26	! 40.4
DRC4 ^a	31.25	! 19.0	50.60	! 25.0
DRC4 ^b	37.86	! 1.84	61.28	! 9.23
DRC4 ^c	39.73	3.01	64.34	! 4.70
DRC4 ^d	39.58	2.62	64.29	! 4.77
Test Program	41.14	6.66	66.42	! 1.61

^a icbrt=2, xmin=0, xmax=9000, ymin=0, ymax=6000, zmin=0, zmax=800, xd=1250, yd=5500, zd=770.04, xo(i)=! 8.1e5, yo(i)=0, zo(i)=0.

^b icbrt=3, xmin=0, xmax=9000, ymin=0, ymax=6000, zmin=0, zmax=800, xd=1250, yd=5500, zd=770.04, xo(i)=! 8.1e5, yo(i)=0, zo(i)=0.

^c icbrt=2, xmin=0, xmax=500, ymin=0, ymax=500, zmin=0, zmax=800, xd=250, yd=250, zd=770.04, xo(i)=! 8.085e5, yo(i)=5250, zo(i)=0.

^d icbrt=2, xmin=0, xmax=500, ymin=0, ymax=500, zmin=0, zmax=500, xd=250, yd=250, zd=250, xo(i)=! 8.085e5, yo(i)=5250, zo(i)=520.04.

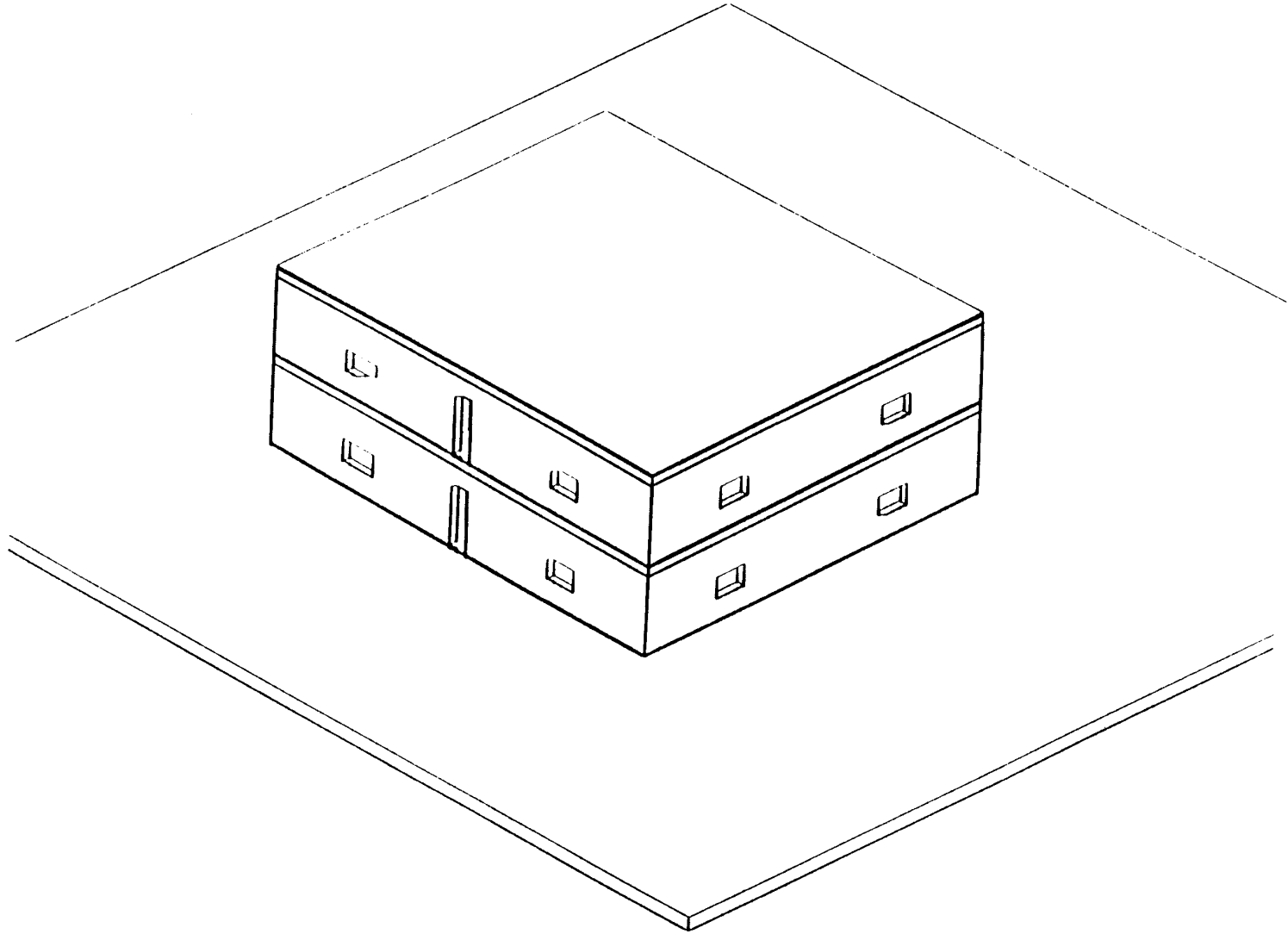


Figure 1. Exterior view of the two-story concrete building used in the DRC3SRF and DRC4 test cases.

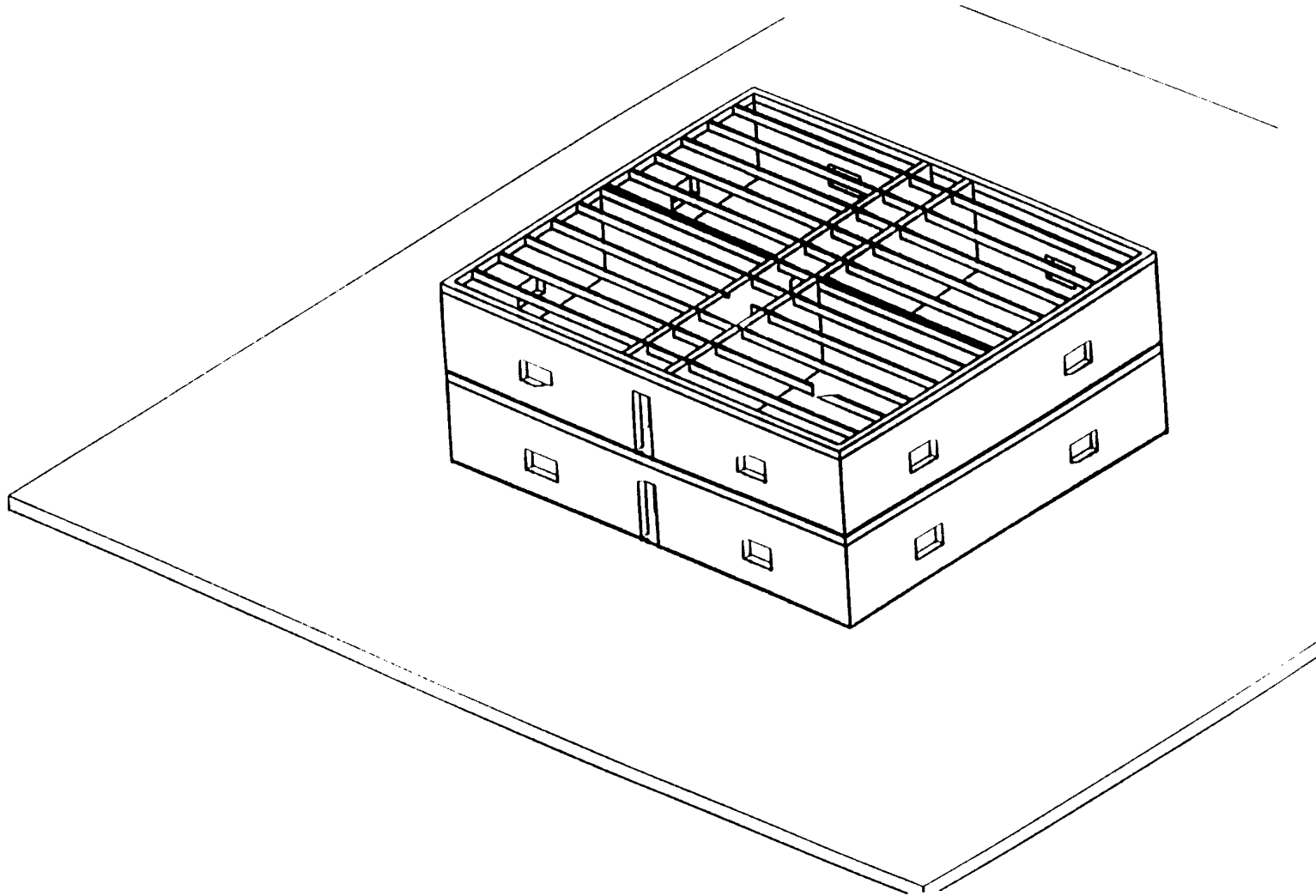


Figure 2. Exterior view of the roofless two-story concrete building used in the DRC3SRF and DRC4 test cases.

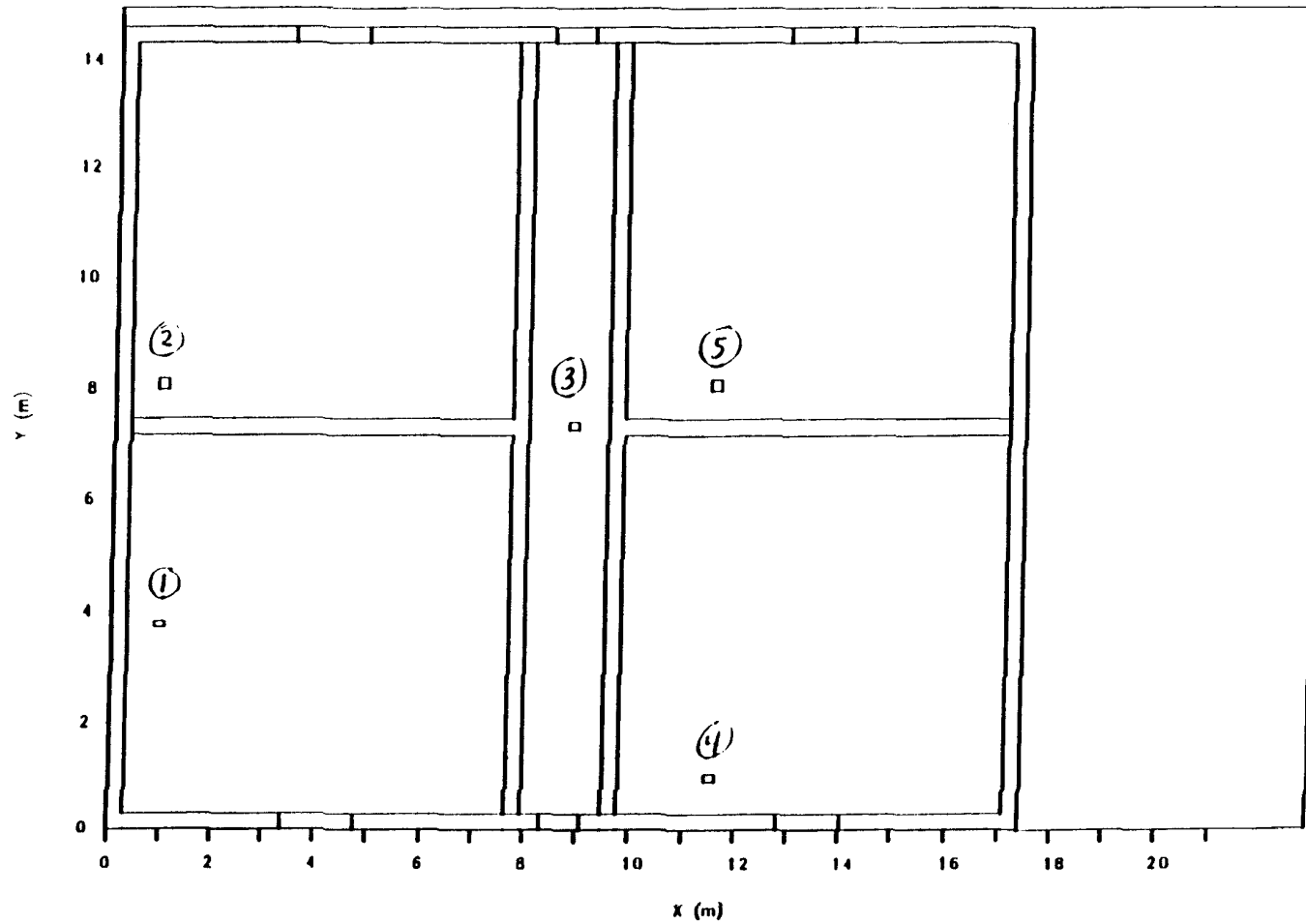


Figure 3. X-Y planar slice through building to show X-Y locations of detectors within the building. The first- and second-floor detectors have the same X and Y coordinates.

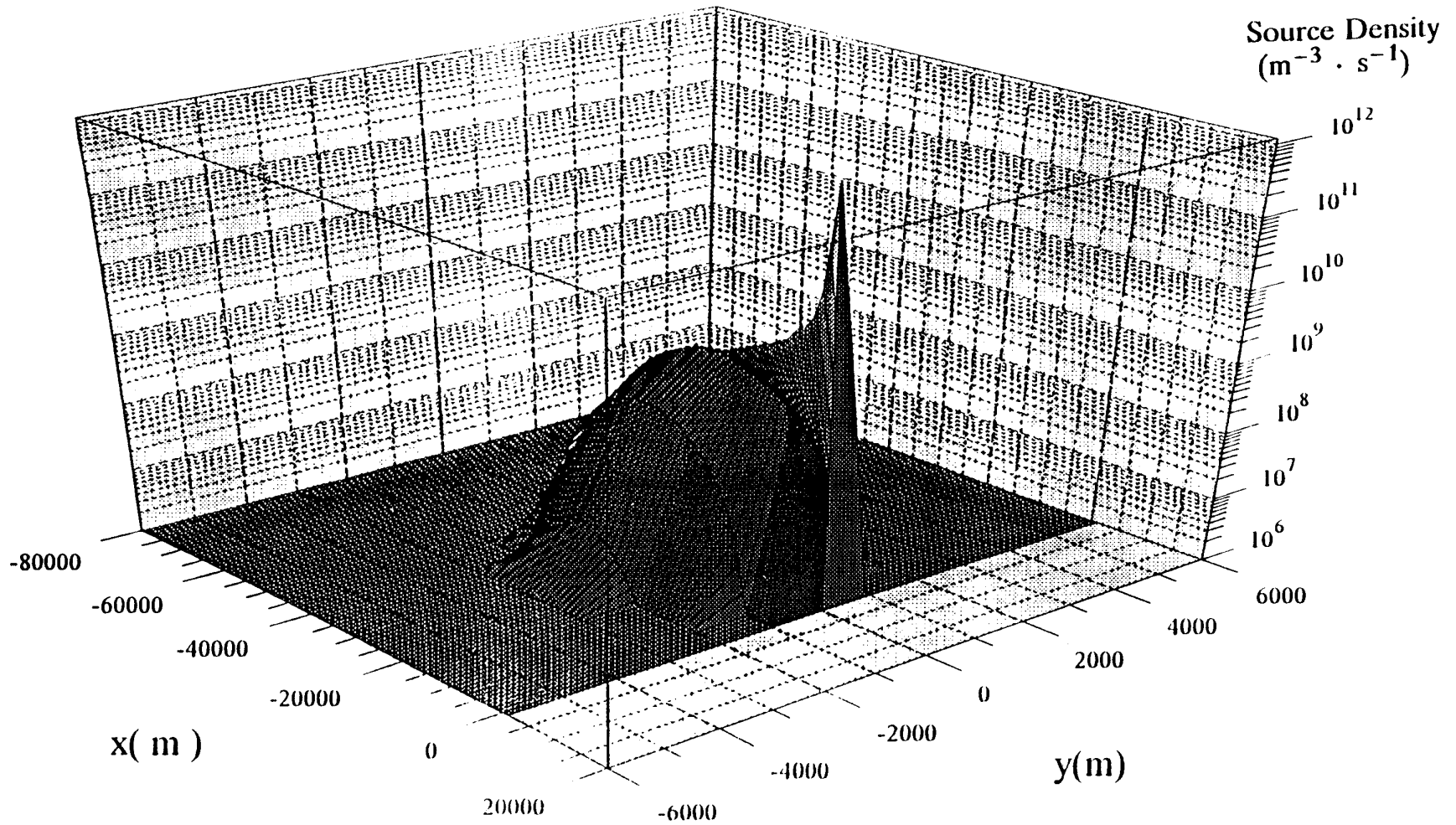


Figure 4. Surface plot of the energy-integrated source ($\text{m}^{13} \text{ @s}^{11}$) at 1-m height one hour after the start of a PWR accident.

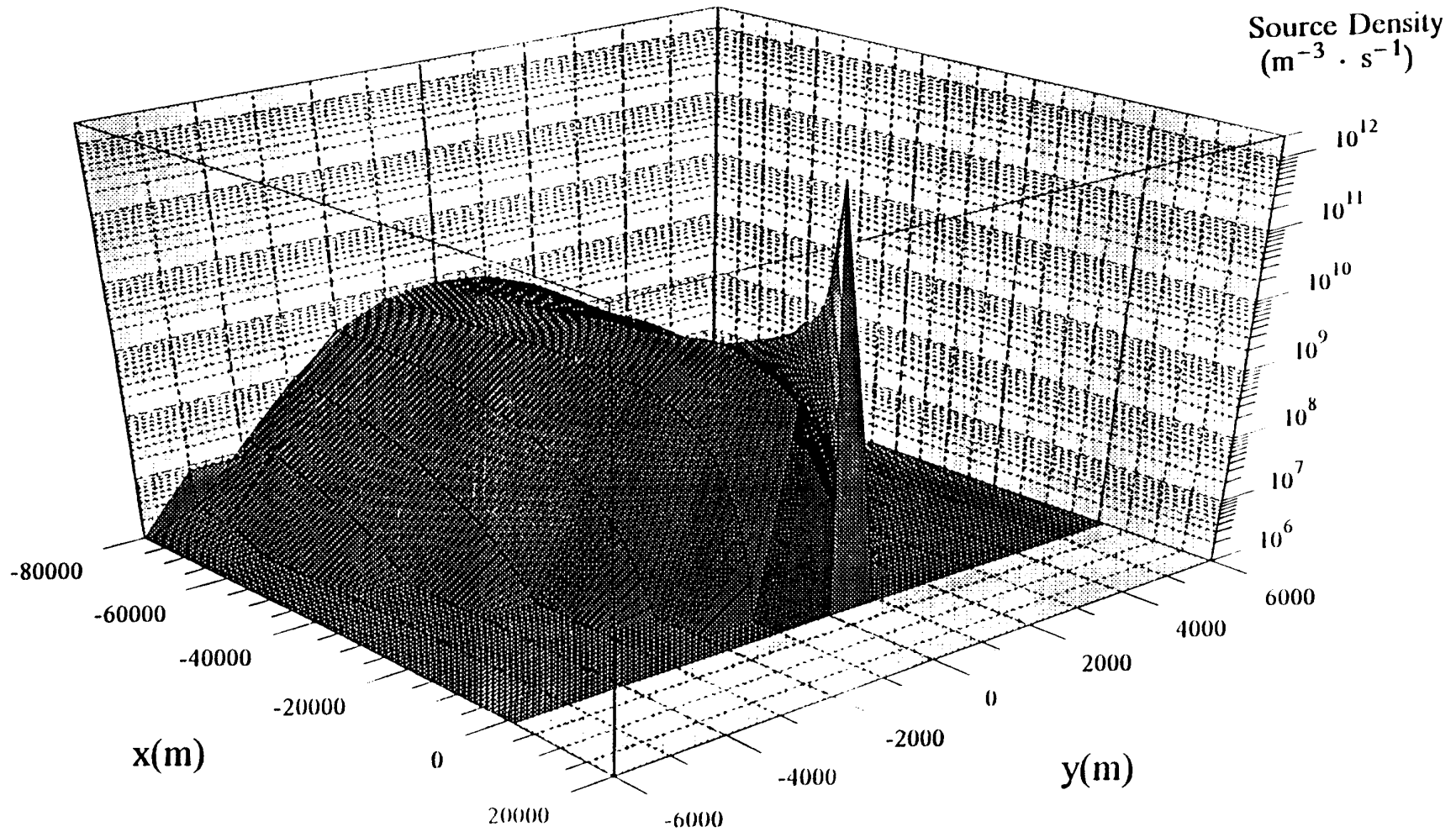


Figure 5. Surface plot of the energy-integrated source (m¹³@s¹¹) at 1-m height three hours after the start of a PWR accident.

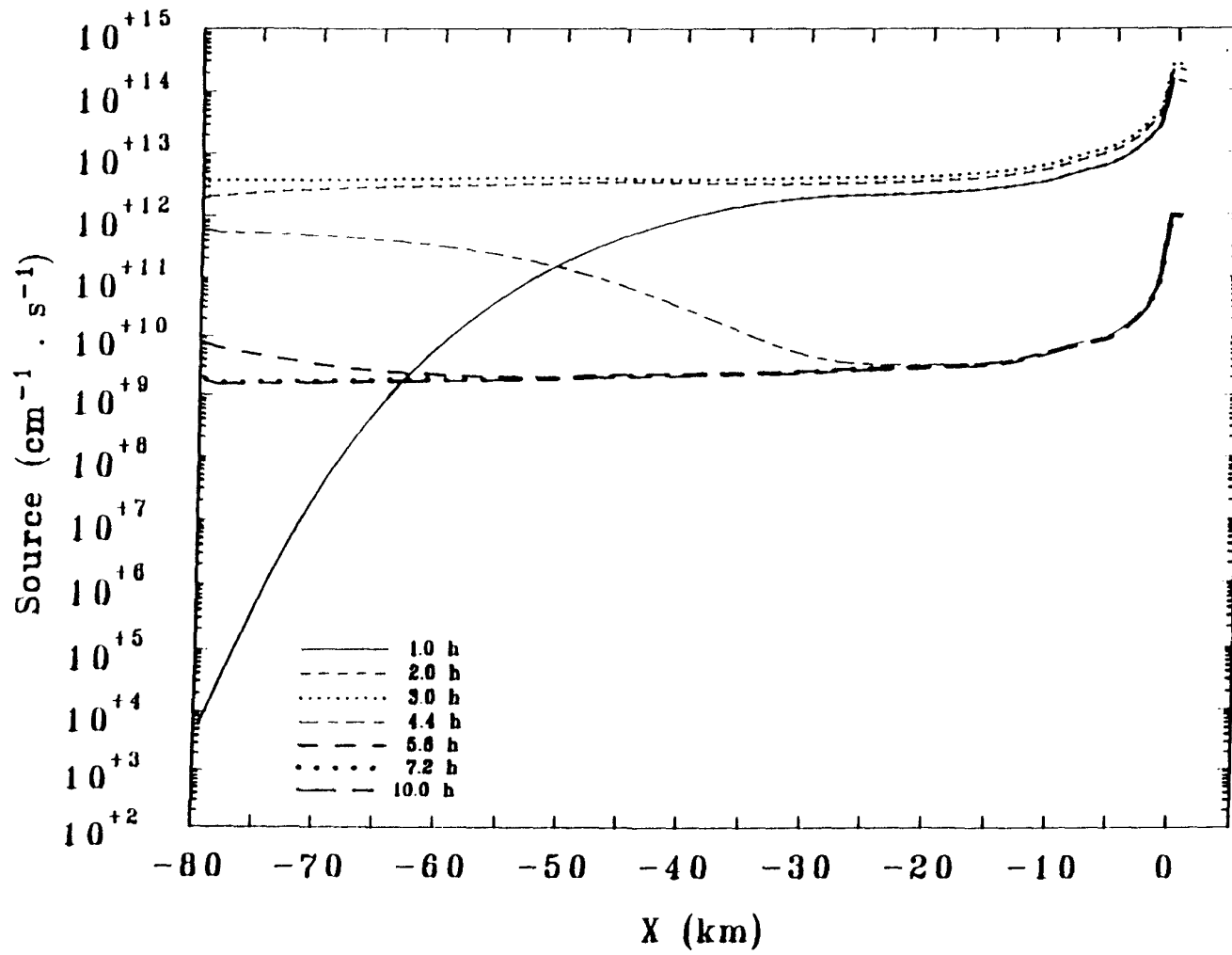


Figure 6. 1-D airborne plume plus ground radiation source distribution as a function of distance along the X-axis.

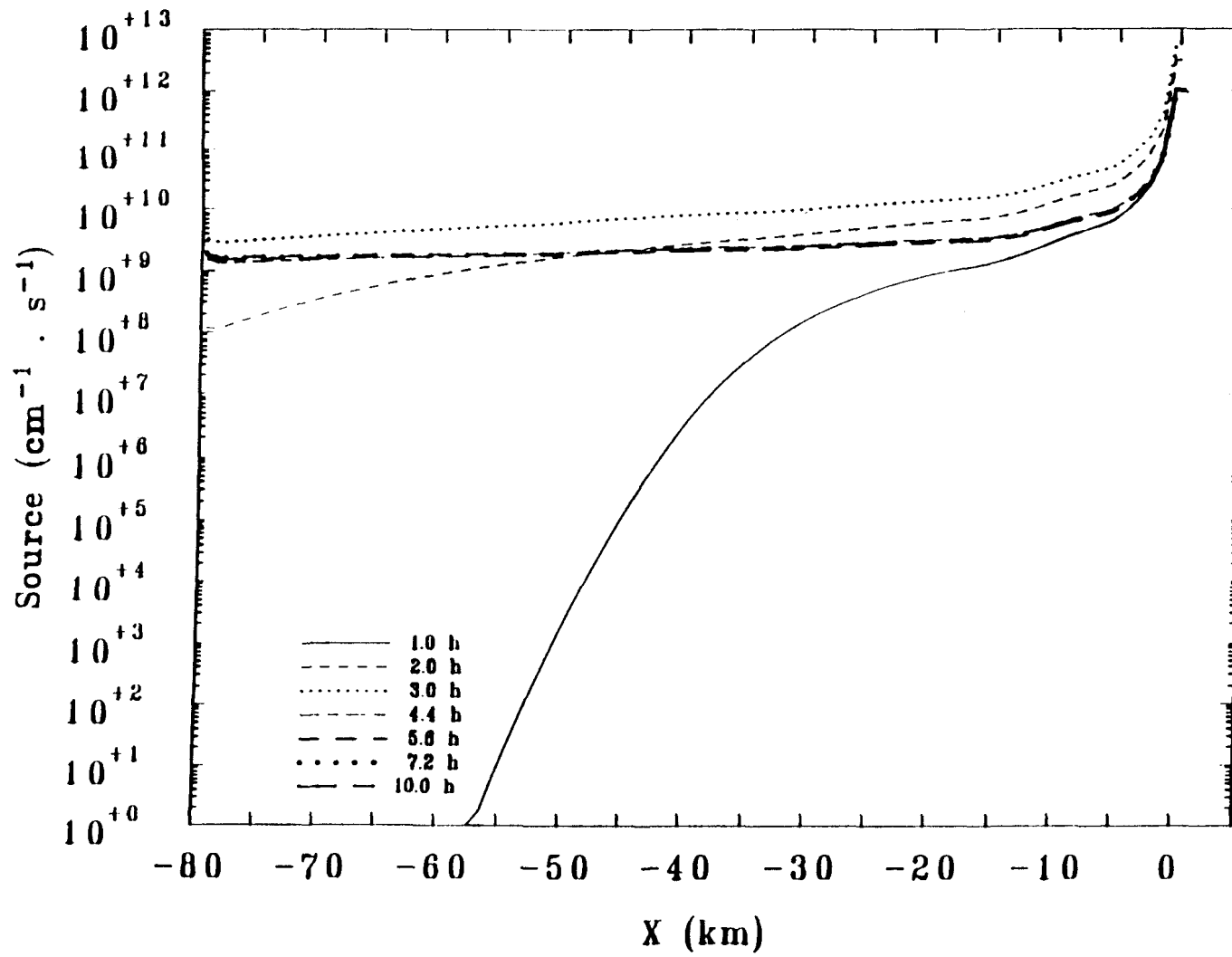


Figure 7. 1-D ground radiation source distribution as a function of distance along the X-axis.

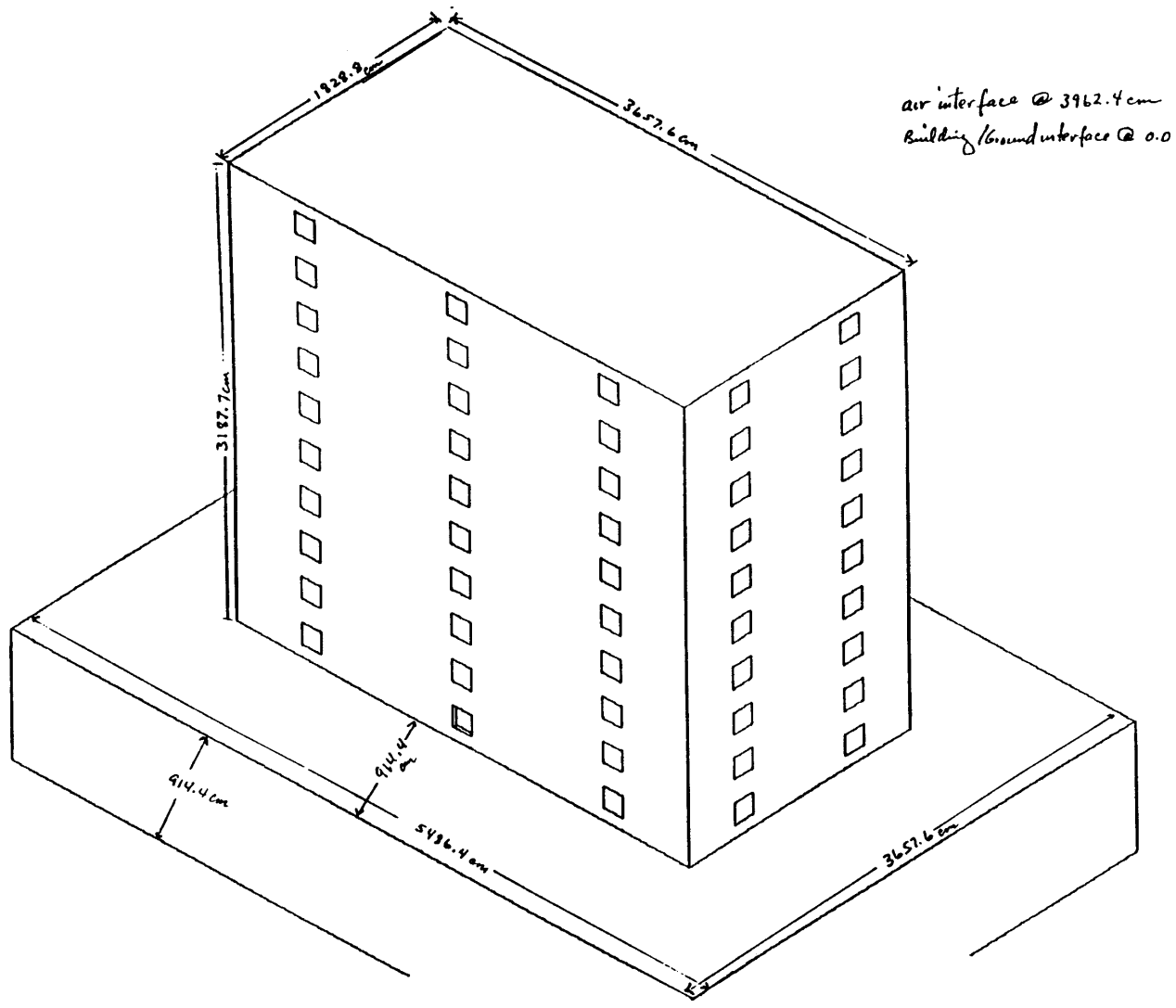


Figure 8. Geometry for the Large, Ten-Story, Thin-Walled, Concrete Building.

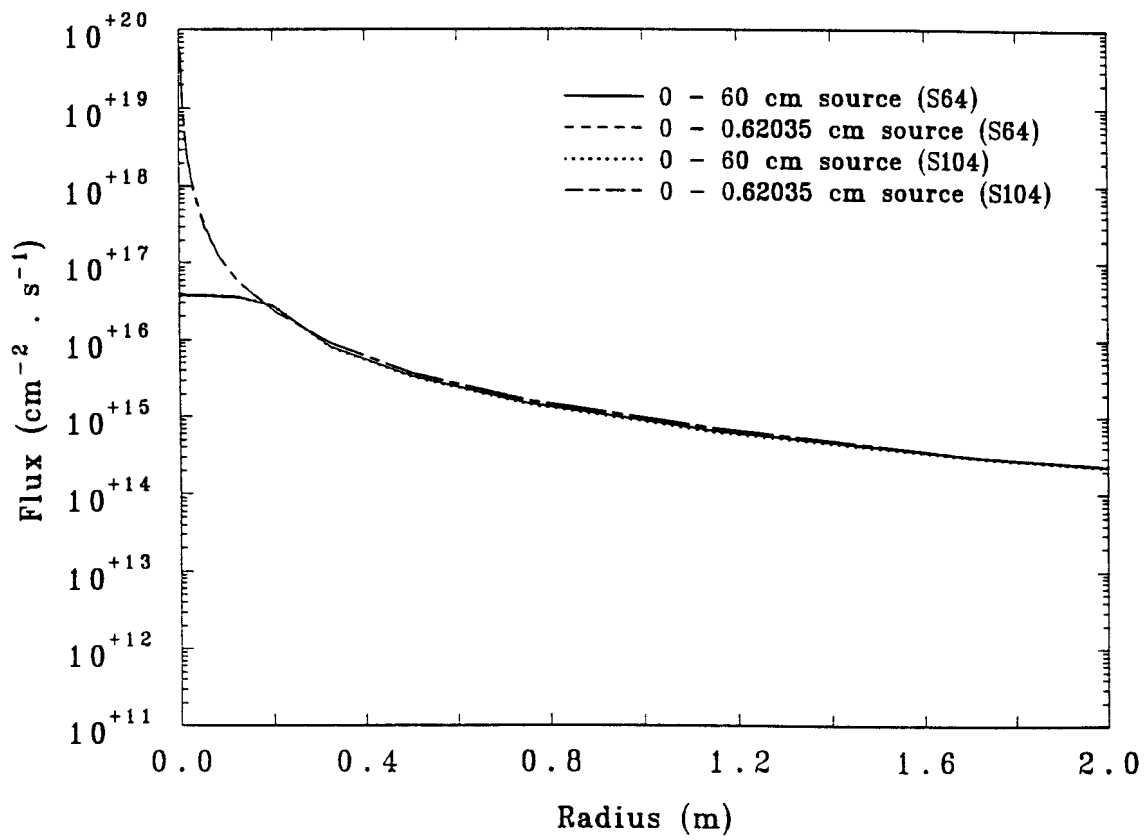


Figure 9. Group 1 fluence spatial distribution as a function of quadrature and point source size.

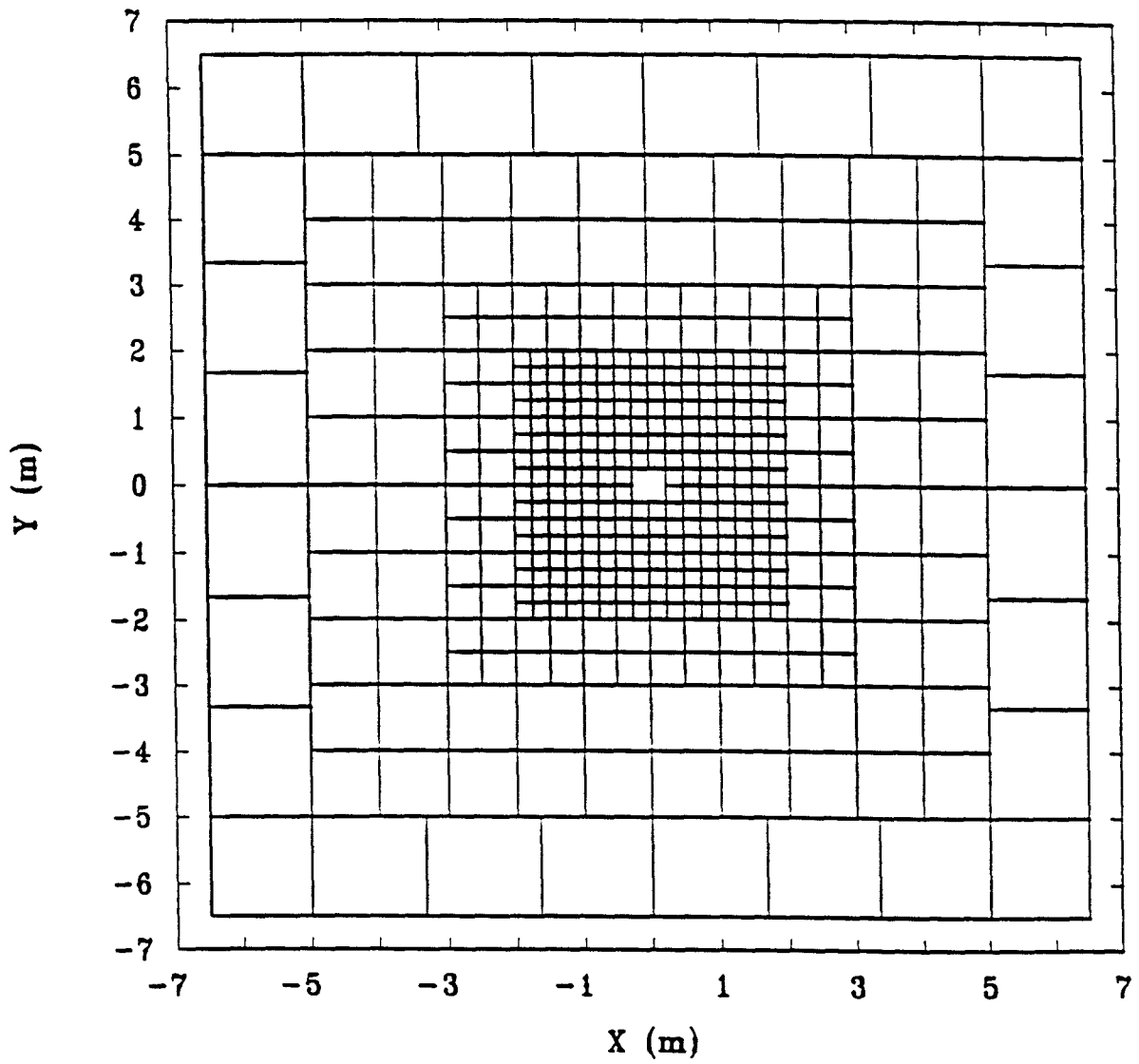


Figure 10. X-Y plane illustration of the original mesh used to integrate plume and surface source contributions to a point at the center of the center box (subdivisions of the first twelve annular regions are shown).

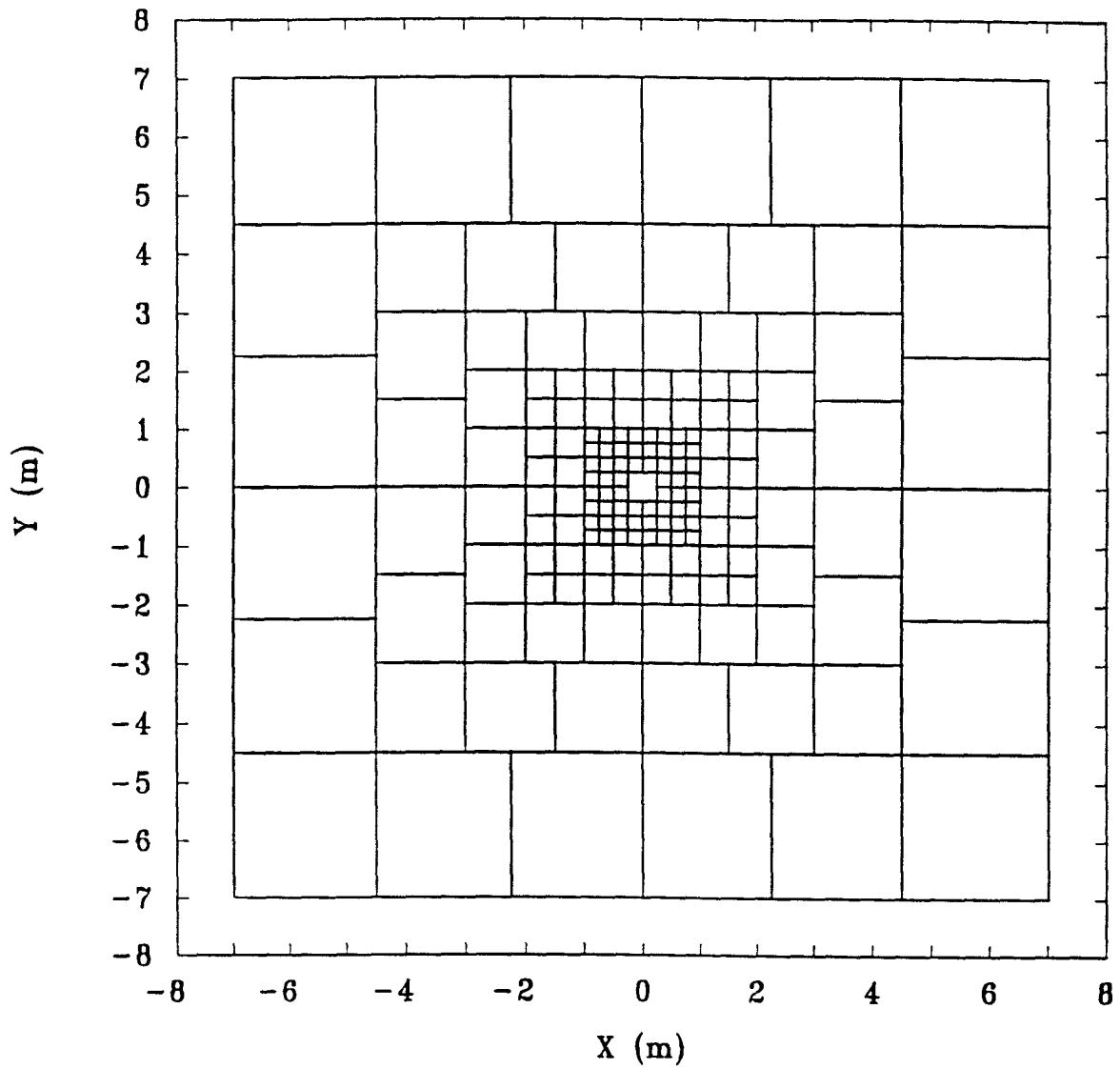


Figure 11. X-Y plane illustration of the revised coarser mesh used to integrate plume and surface source contributions to a point at the center of the center box (subdivisions of the first eight annular regions are shown).

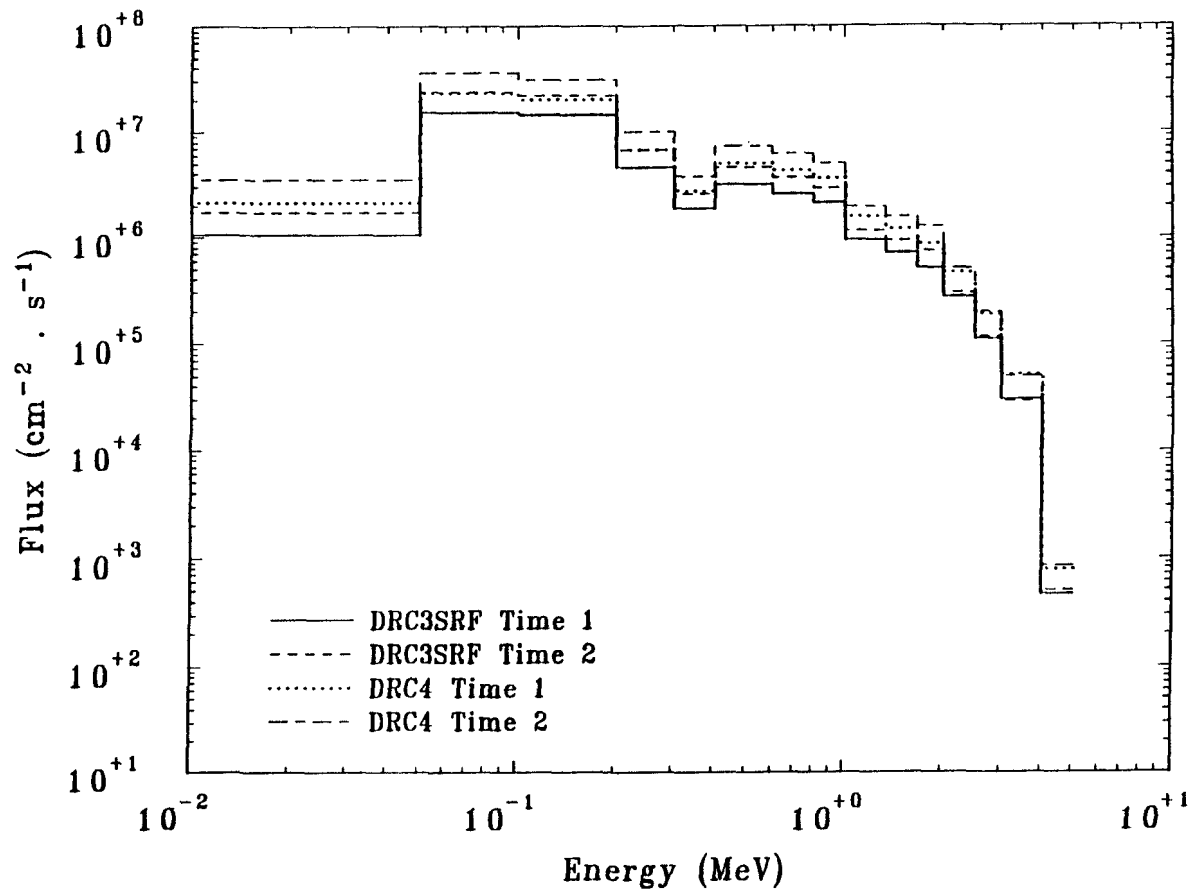


Figure 12. Comparison of DRC3SRF and DRC4 free-field fluence spectra at detector position 1 in a two-story building for two time steps.

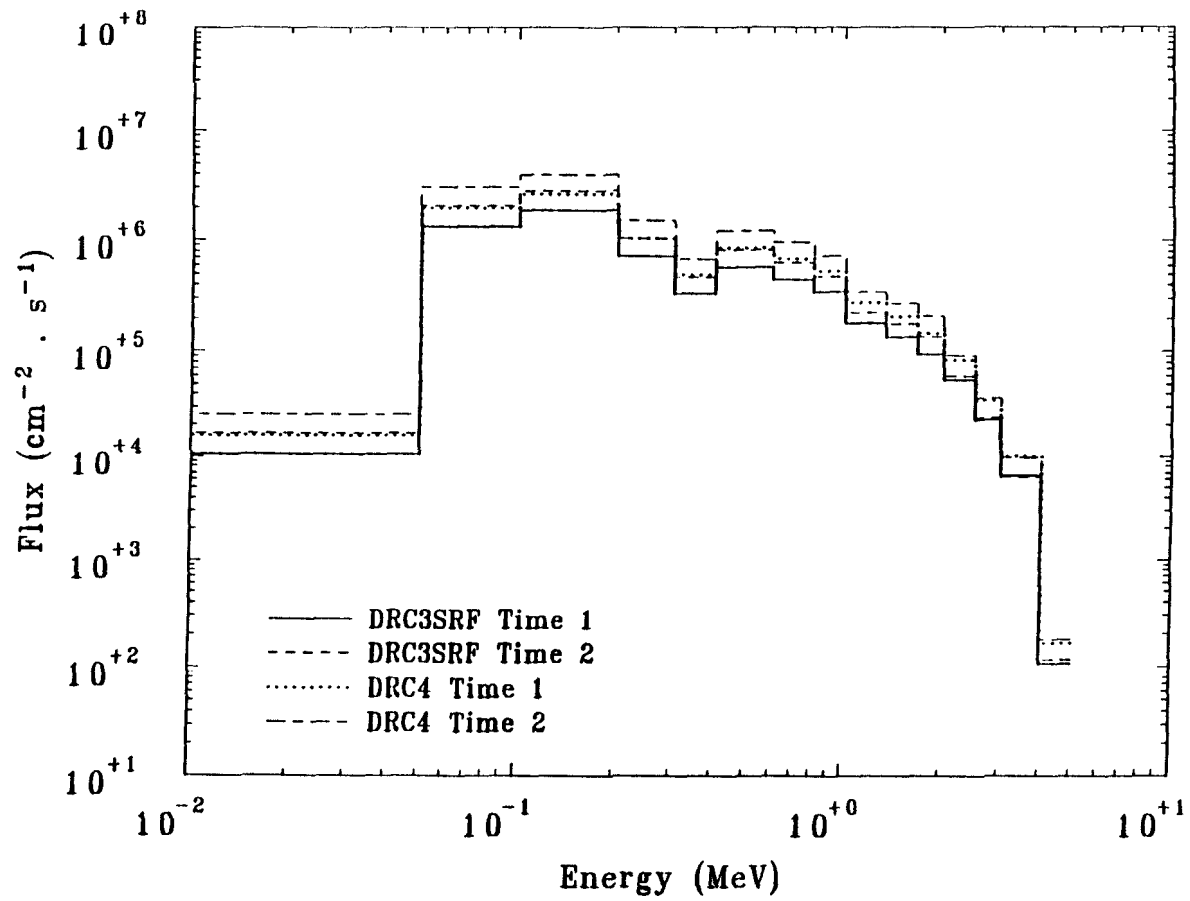


Figure 13. Comparison of DRC3SRF and DRC4 shielded fluence spectra at detector position 1 in a two-story building for two time steps.

APPENDIX A

INPUT INSTRUCTIONS FOR VARIOUS CODES

APPENDIX A

INPUT INSTRUCTIONS FOR VARIOUS CODES

A.1 Input Instructions for DRC4

The following input instructions are patterned after draft documentation written by M. B. Emmett for the DRC code and on documentation for the DRC2 and DRC3 codes. The DRC4 code was created from the DRC3SRF code, and it has provisions for coupling with DORT fluences (i.e. it performs the functions of DRC2), with TORT surface fluences (i.e. it performs the functions of DRC3SRF), as well as with plume source directional fluences calculated in point-kernel manner from GENMASH energy- space- and time-dependent plume sources. One option of the DRC4 code (idos=3) eliminates one or more steps in the coupling procedure. For example, the DORT fluences are processed with VISTA, the TORT fluences are processed with the VIST3DP code, but no such processing is required by the idos=3 option in DRC4. In the input instructions, the term "vehicle" is used to refer to an object or a structure that perturbs the air-over-ground radiation field. It is modeled in the localized MASH-MORSE calculation. A "vehicle system" includes the object and the air and ground modeled in the MASH-MORSE calculation.

Input Card A: (20a4) Title for this problem.

Input Card B: Free-form FIDO format - Begin with '***' in columns 2 and 3.

1. xd - x-location (cm) of the detector in MASH-MORSE geometry.
2. yd - y-location (cm) of the detector in MASH-MORSE geometry.
3. zd - z-location (cm) of the detector in MASH-MORSE geometry.
4. zbot- bottom of coupling surface relative to MASH-MORSE geometry (cm).
5. ztop- top of coupling surface relative to MASH-MORSE geometry (cm).
6. ipt - printout options
 - 0 = print VISTA or VIST3DP file control data and vehicle doses
 - 1 = print VISTA or VIST3DP file control data and free-field spectra
 - 2 = print VISTA or VIST3DP file control data, free-field spectra, vehicle doses and dose spectra,

and protection factors

- 3 = print VISTA or VIST3DP file control data , vehicle doses, and protection factors.
(Note: iprt must be 2 for unit 10 output).
7. watmx - maximum adjoint particle weight accepted.
 8. ndet- number of vehicle range/orientations.
 9. idif - 0/>0 = same/different group structures for MASH-MORSE and VISTA data or MASH-MORSE and VIST3DP data.
 10. ksiz- k-words of storage to be allocated (0 uses the default size of 100k words). Actually, ksiz is not used. The total storage, maxsz, is fixed at 10,000,000. The value for maxsz should be set to a smaller number for machines with less available core storage.
 11. ibufsz - MASH-MORSE collision file record length in words (1625).
 12. nparm- number of parameters written on collision file (13).
 13. idxy - 0 = no x-y data on collision file
 - 1 = x-y data on collision file but no x-y dependence in the coupling calculation
 - 2 = x-y data on collision file and x-y dependence in the coupling calculation
(Note: if idos=2 or 3, idxy has no effect).
 14. iww - number of responses desired (less than or equal to 10. Note that a iww=0 implies 2 responses and iww must be > 0 for unit 11 to be written).
 15. xq - x-location (cm) of the vehicle system rotation point relative to MASH-MORSE geometry.
 16. yq - y-location (cm) of the vehicle system rotation point relative to MASH-MORSE geometry.
 17. interp - 1/2 = linear/exponential fluence interpolation.
 18. xnorm- response multiplier (default=1.0).
 19. idos - 1/2/3 = directional fluences result from DORT/TORT/GENMASH.
 20. nscflx - for idos=2, TORT scalar fluence file unit number if > 0.

21. ifall- for idos=3, 0/1=no effect/include directional fluences from fallout on top of structure.
22. xmin - for idos=3, minimum x (cm) in MASH-MORSE for structure.
23. xmax - for idos=3, maximum x (cm) in MASH-MORSE for structure.
24. ymin - for idos=3, minimum y (cm) in MASH-MORSE for structure.
25. ymax - for idos=3, maximum y (cm) in MASH-MORSE for structure.
26. zmin - for idos=3, minimum z (cm) in MASH-MORSE for structure (most likely set to the minimum z for GENMASH).
27. zmax - for idos=3, maximum z (cm) in MASH-MORSE for structure.
28. kyold - for idos=3, 0/1/2=no effect/write DRC4 directional fluences to unit noldq/read previously-calculated DRC4 directional fluences from unit noldq.
29. qmin - for idos=3, value below which the GENMASH source value is set to zero.
30. mpts - for idos=3, number of points in each spatial direction on a box surrounding the target structure at which DRC4 directional fluences will be calculated for each space-time/orientation (2 appears to be sufficient and calculation time increases exponentially with increases in mpts).

(Note: all the above parameters are input as real numbers and are converted to integers where required).

Input Card C: If idos=3, the four-character name of the 3-D quadrature set used to bin the DRC4 directional fluences.

Input Card D: Ranges, vehicle-system/source-system z-offsets, and orientation arrays - Free-form FIDO format - Begin with '***' in columns 2 and 3.

Ranges: $(x_o(i), i=1, n_{det})$ (cm) - DORT radii or TORT or GENMASH x-distance to the vehicle system rotation point for each case.

Ranges: $(y_o(i), i=1, n_{det})$ (cm) - TORT or GENMASH y-distance to the vehicle system rotation point for each case (set to 0.0 for idos=1).

MASH-MORSE-DORT, MASH-MORSE-TORT, or MASH-MORSE-GENMASH z-offsets: $(z_o(i), i=1, \text{ndet})$ - DORT, TORT, or GENMASH ground-air interface z-location (cm) minus MASH-MORSE ground-air interface z-location (cm). For simplicity, the MASH-MORSE ground-air interface should be placed at $z=0.0$. Then one need only specify the locations of the DORT, TORT, or GENMASH ground-air interface.

time values at which GENMASH directional fluences are to be calculated: $(t_o(i), i=1, \text{ndet})$ (GENMASH source file time units) - there is a provision for interpolation between the GENMASH source times. (always input but used only if $\text{idos}=3$).

Orientation array: $(\alpha(i), i=1, \text{ndet})$ - orientation angles (degrees counterclockwise) of the vehicle system with respect to the positive portion of the DORT, TORT, or GENMASH system x-axis.

Input Card E: (if $\text{idif} > 0$) $\text{nneut}, \text{ngam}$ - Free-form FIDO format - Begin with in columns 2 and 3. (input is not necessary if $\text{idos}=3$, energies are obtained from the GENMASH file).

nneut - group number of lowest energy neutron group in VISTA or VIST3DP.

ngam - group number of lowest energy photon group in VISTA or VIST3DP.

Input Card F: (if $\text{idif} > 0$) VISTA or VIST3DP energy group boundaries ($\text{nog}+2$ entries).^c Free-form FIDO - Begin with '***' in columns 2 and 3. Enter neutron upper energy boundaries in descending order followed by photon upper energy boundaries in descending order followed by the lower energy boundaries of the ' ngam ' photon group and the ' nneut ' neutron group.

Input Card G: (20a4) Alphanumeric Title Information.

Input Card H: (20a4) Title or units for total responses for all detectors.

Input Card I: (20a4) Title or units for each total response nr .

Input Card J: Response Function nr - Free-form FIDO format - Begin with '***' in columns 2 and 3.

$(\text{resp}(i, \text{nr}), i=1, \text{nmtg})$ - enter values in order of decreasing energy.

Repeat Cards I and J for each response function.

^c nog is read from the VISTA or VIST3DP file and is the number of groups for which data is provided on the file.

Input Card K: (20a4) Title or units for energy dependent fluence.

To run additional cases, respecify all cards.

A.2 Input Instructions for GENTORT

1. Problem Title (18a4 format)
2. up to 30-character name for local file linked to the TORT input file
3. Block 1 input.

0* Array [11 entries]

txo TORT origin x-location relative to plume source geometry

tyo TORT origin y-location relative to plume source geometry

tzo TORT origin z-location relative to plume source geometry

tang TORT geometry orientation relative to the plume source geometry

zgrndTORT z-location of the ground surface

xlo TORT minimum x extent of building

xhiTORT maximum x extent of building

ylo TORT minimum y extent of building

yhiTORT maximum y extent of building

zloTORT minimum z extent of building

zhiTORT maximum z extent of building

1\$ Array [5 entries]

nqin unit number for the GENMASH source file

kittime step at which source is selected

npctr 0/1=no effect/print sources at key positions (specified in TORT input)

interp1/2=use linear/exponential interpolation

ipert 0/>0=no effect/zero source in region occupied by building

End of Block 1. End with a "t".

A.3 Input Instructions for PLATEQ

1. Problem Title (18a4 format)

2. Block 1 Input

0\$ Array [14 entries]

nplate unit number for output plateout source file

nplume unit number for plume source input file

igm number of output energy groups

im number of i-intervals for TORT calculation

jm number of j-intervals for TORT calculation

km number of k-intervals for TORT calculation

i1 first i-patch interval for TORT calculation

i2 last i-patch interval for TORT calculation

j1 first j-patch interval for TORT calculation

j2 last j-patch interval for TORT calculation

k1 first k-patch interval for TORT calculation

k2 last k-patch interval for TORT calculation

it selected time step for which plateout source is output

1* Array [3 entries]

xc x-position of TORT origin in plume source geometry

yc y-position of TORT origin in plume source geometry

ang angle (deg.) by which the TORT geometry is rotated in the plume source geometry

End of Block 1. End with "t".

3. Block 2 input

2* Array [im+1 entries] - TORT geometry x-boundaries.

3* Array [jm+1 entries] - TORT geometry y-boundaries.

4* Array [km+1 entries] - TORT geometry z-boundaries.

5* Array [igm+2 entries] - output energy-group boundaries (eV) from high to low energies:
(eo(ig),ig=1,igm+2).

End of Block 2. End with "t".

A.4 Input Instructions for VIST3DP

Problem Title (20a4 format)

1\$ Array [8 entries]

nuncfunit number for the input TORT uncollided scalar fluence file (if > 0). This file is for the full TORT geometry.

nflsv unit number for the input TORT scalar fluence file.

nuncaunit number for the input uncollided boundary fluence file (if > 0).

naft unit number for the input boundary fluence file from TORT/TORSET.

nflo unit number for the output patch geometry scalar fluence file.

nafo unit number for the output boundary fluence file for coupling with DRC3SRF.

nplate unit number for input isotropic plateout source (created by program PLATEQ).

nafo2unit number for an output boundary fluence file for TORT (if >0, otherwise use source from naft).

End of Block 1. End with a "t".

81* Array [mm values] weights for 3-D quadrature selected for TORSET.

82* Array [mm values] mu values for 3-D quadrature selected for TORSET.

83* Array [mm values] eta values for 3-D quadrature selected for TORSET.

End of Block 2. End with a "t".

A.5 Input Instructions for QUAD3D

1. Problem Title [18a4 format]

2. Block 1 Input

1\$ Array [2 entries]

nquad number of 3-D quadrature sets to be processed

ntq unit number for the quadrature output file

End of Block 1. End with a "t".

3. four-character names for the quadrature sets [format (14(a4,1x))]

4. Block 2 Input

2\$ Array [nquad entries] - mmq array: number of directions in each quadrature set

End of Block 2. End with a "t".

5. Blocks 3 Through nquad+2 Input - 3-D quadrature data from unit 10^d

do nq=1,nquad

Read the following block of data:

81* Array [mmq(nq) entries] - 3-D quadrature weights for set nq

82* Array [mmq(nq) entries] - 3-D quadrature mu values for set nq

83* Array [mmq(nq) entries] - 3-D quadrature eta values for set nq

End of Block nq+2. End with a "t".

enddo

^dThe initial quadrature data file consists of the TORT quadrature file sncon3d minus the S_6 and smaller quadrature sets and the LANL quadrature sets. The total number of remaining sets is 13.

A.6 Input Instructions for G2GAIR

1. Problem Title [18a4 format]

2. Block 1 Input

1\$ Array [9 entries]

igm number of energy groups in ANISN calculations

im number of intervals in ANISN calculations

imo number of output locations for output angular fluence data

isn number of nonzero-weight angles in the ANISN quadrature

jgskp number of groups for which data will be skipped on each ANISN fluence file

nt1 unit number for the first ANISN angular fluence file

nt2 unit number for the output fluence file

ism number of angles in the output quadrature

neut number of neutron groups. (If neut > 0, the output number of neutron groups will be different from neut if jgskp > 0)

2* Array [2 entries]

constm constant multiplier that normalizes the ANISN angular fluences^e

rref reference r from which to calculate distances from the source to various detectors (a value equal to half the point-source radius is recommended)

End of Block 1. End with a "t".

3. Block 2 Input

^econstm is the inverse of a constant used in ANISN to keep calculated fluxes within the allowable range of real numbers on the IBM RISC workstations.

3* Array [im+1 entries] - spatial mesh boundaries for ANISN calculations

4* Array [isn+1 entries] - ANISN 1-D quadrature cosines

5* Array [isn+1 entries] - ANISN 1-D quadrature weights

6* Array [imo entries] - spatial locations at which fluences will be output

7\$ Array [isn+1 entries] - output quadrature angles corresponding to input quadrature (use 0 for the zero-weight angle)

8* Array [igm+2 entries] - energy group top boundaries from high to low followed by the bottom energy boundaries of groups igm and neut3

End of Block 2. End with a "t".

Cases may be stacked by respecifying input at steps 1-3.

APPENDIX B

DESCRIPTIONS OF FILES USED OR CREATED BY VARIOUS CODES

APPENDIX B

DESCRIPTIONS OF FILES USED OR CREATED BY VARIOUS CODES

B.1 DRC4 Directional Fluence File Format

Record 1: mm - number of directions in 3-D quadrature used to bin fluences

Record 2: (cosl(m),m=1,mm),(cosu(m),m=1,mm),(phil(m),m=1,mm),(phiu(m),m=1,mm),
(wts(m),m=1,mm),(amu(m),m=1,mm),(eta(m),m=1,mm),(xzi(m),m=1,mm),
(((smesh(i,k,jdet),i=1,3),k=1,kpts),jdet=1,ndet)

Records 3 through nmtg*ndet+2:

```
do ig=1,nmtg
  do jdet=1,ndet
    ((flxm(m,k,jdet,ig),m=1,mm),k=1,kpts)
  enddo
enddo
```

Notes:

cosl and cosu are the lower and upper polar cosine boundaries of the 3-D quadrature solid angles, and phil and phiu are the lower and upper azimuthal angle boundaries of the 3-D quadrature solid angles. wts, amu, eta are the quadrature components input to TORT and xzi are the computed y-direction cosines. kpts is the number of fluence points surrounding the structure for each of the ndet space-time/orientations that the user specifies. nmtg is the number of energy groups, and the flxm array contains the directional fluences. This file is written if kyold=1 and is read if kyold=2; there is no effect if kyold=0. The fluences from this file are valid for changes in the MASH-MORSE adjoint source location or changes in the orientation of the structure. However, ndet in follow-on cases must be the same as that for the initial case.

B.2 GENMASH Source File Format

Record 1: nx, ny, nz, nng, ngg, nit, jmesh

Record 2: (sx(i),i=1,nx),(sy(i),i=1,ny),(sz(i),i=1,nz)

Record 3: (eb(ig),ig=1,nng+1),(eb(nng+1+ig),ig=1,ngg+1)

Record 4: (t(it),it=1,nit)

Records 5 through (nz+1)*nit+4:

```
do it=1,nit
  do k=1,nzz+1
    (((plumeq(ig,i,j),ig=1,nog),i=1,nxx),j=1,nyy)
  enddo
enddo
```

Notes:

nx, ny, and nz are the number of x, y, and z source mesh, respectively. nng and ngg are the number of neutron and photon groups and nit is the number of time steps. jmesh tells whether the source file data are mesh-centered (jmesh=1) or mesh-edged (jmesh=0). nxx=nx, nyy=ny, and nzz=nz for jmesh=0, and nxx=nx-1, nyy=ny-1, and nzz=nz-1 for jmesh=1. sx, sy, and sz are the x, y, and z source mesh boundaries (jmesh=1) or source locations (jmesh=0). The source is ordered by k-plane and time on the file with the first k-plane being the ground source and k-planes 2 through nz+1 being the airborne source.

B.3 GENTORT Output File Format

This is a source moments file in the TORT VARMOM format. The VARMOM file format was developed by R. A. Lillie of ORNL, and it takes almost all of its structure from the 2-D DORT VARSOR file format and the 3-D TORT FLXMOM and VARSCL file formats. It was created to allow discontinuous mesh distributed source data to be written to a file which could then be read by the current version of TORT. The structure of this file format follows:

```
C
C
C*****
C
C                                20 MAY 97
C
CF VARMOM
CE VARIABLE MESH CELL-AVERAGE DATA
C
C*****
C
CC ORDER OF GROUPS IS BY DECREASING ENERGY;
CC NEUTRONS THEN PHOTONS - REVERSE IF ADJOINT
CC I IS THE FIRST -DIMENSION INDEX
CC J IS THE SECOND -DIMENSION INDEX
CC K IS THE THIRD -DIMENSION INDEX
CC IMA=IABS(IM)
C
CC MULT=1 IF WORD LENGTH IS 8 BYTES; MULT=2 IF 4 BYTES
C
CC WHEN IM.GT.0, THE MESH IS REGULAR (CONTINUOUS) WITH
CC IM CELLS IN EACH ROW AND JM ROWS IN EACH PLANE,
CC ISM=JSM=KSM=1. IMS=IM, JMS=JM.
C
CC WHEN IM.LT.0, THE MESH IS DISCONTINUOUS, EACH PLANE
CC CONTAINS JMS ROWS, WHERE JMS=JMBJS(JSET(K)). EACH
CC ROW CONTAINS IMS CELLS, WHERE IMS=IMBIS(ISET(JMK)).
CC (JMK) DENOTES J + SUM OF JMS(KK) OVER KK=1,...,K-1.
C
CC CELL AVERAGE RESPONSE DATA USES IFMOM=1, IFBND=0, LM=0.
C
CC DISTRIBUTED SOURCE MOMENT DATA USES IFMOM=1, IFBND=0,
CC LM>0.
C
CC CELL AVERAGE FLUX MOMENT DATA USES IFMOM=1, IFBND=1,
CC LM>0. (AT PRESENT TIME, DUMMY RECORDS ARE WRITTEN
CC FOR THE BOUNDARY FLUX DATA)
```

```

C-----
-----
CS  FILE STRUCTURE
C
CS  RECORD TYPE                PRESENT IF
C  -----                    -----
CS  FILE IDENTIFICATION        ALWAYS
CS  FILE LABEL                  ALWAYS
CS  INTEGER PARAMETERS          ALWAYS
CS  INDEXING ARRAYS             ALWAYS
CS  REAL ARRAYS                 ALWAYS
C
CS  * ***** REPEAT OVER ALL RESPONSES (NRESP)
CS  *
CS  *   CELL RESPONSE DATA      IF IFMOM.GT.0 AND LM.EQ.0
CS  *
CS  * *****
C
CS  * ***** REPEAT OVER ALL GROUPS (IGM)
CS  *
CS  *   ***** REPEAT OVER ALL ROWS (JMSKM)
CS  * *
CS  * *   CELL MOMENT DATA      IF IFMOM.GT.0 AND LM.GT.0
CS  * *
CS  * *****
CS  *
CS  *   I-BOUNDARY DIRECTIONAL DATA  IF IFBND.GT.0
CS  *   J-BOUNDARY DIRECTIONAL DATA  IF IFBND.GT.0
CS  *   K-BOUNDARY DIRECTIONAL DATA  IF IFBND.GT.0
CS  *
CS  * *****
C
CS  * ***** REPEAT OVER ALL GROUPS (IGM)
CS  *
CS  *   ***** REPEAT OVER ALL PLANES (KM)
CS  * *
CS  * *   UNCOLLIDED SCALAR FLUXES    IF ISOP.EQ.1
CS  * *
CS  * *****
CS  *
CS  * *****
C
C-----
-----
C

```

C

C-----

CR FILE IDENTIFICATION

C

CL HNAME,(HUSE(I),I=1,2),IVERS

C

CW NUMBER OF WORDS= 4*MULT

C

CD HNAME

FILE NAME

CD HUSE(I)

USER IDENTIFICATION

CD IVERS

FILE VERSION NUMBER

C

C-----

C

C

C-----

CR FILE LABEL

C

CL DATE,USER,CHARGE,CASE,TIME,(TITL(I),I=1,12)

C

CW NUMBER OF WORDS= 17*MULT

C

CD DATE

AS PROVIDED BY TIMER OPTION 4 - (A6)

CD USER

AS PROVIDED BY TIMER OPTION 5 - (A6)

CD CHARGE

AS PROVIDED BY TIMER OPTION 6 - (A6)

CD CASE

AS PROVIDED BY TIMER OPTION 7 - (A6)

CD TIME

AS PROVIDED BY TIMER OPTION 8 - (A6)

CD TITL(I)

TITLE PROVIDED BY USER - (A6)

C

C-----

C

C

C-----

CR INTEGER PARAMETERS

C

CL IGM,IM,JM,KM,IZM,NEUT,ISM,JSM,IMSISM,JMSJSM,JMSKM,NCONV,NJBLK,

CL LM,NRESP,IFMOM,IFBND,ISOP,(IDUM(I),I=1,7)
 C
 CW NUMBER OF WORDS= 25
 C
 CD IGM NUMBER OF ENERGY GROUPS
 CD IM MAXIMUM NUMBER OF CELLS IN ANY ROW
 CD JM MAXIMUM NUMBER OF ROWS IN ANY PLANE
 CD KM NUMBER OF PLANES
 CD IZM NUMBER OF MATERIAL ZONES
 CD NEUT NUMBER OF NEUTRON GROUPS
 CD (IGM IF ALL NEUTRONS, 0 IF ALL PHOTONS)
 CD ISM NUMBER OF ISETS
 CD JSM NUMBER OF JSETS
 CD IMSISM SUM OF IMS OVER ALL ISM
 CD JMSJSM SUM OF JMS OVER ALL JSM
 CD JMSKM SUM OF JMS OVER KM (TOTAL NO. OF ROWS)
 CD NCONV NUMBER OF LAST GROUP CONVERGED
 CD NJBLK NUMBER OF SPACE MESH BLOCKS PER GROUP
 CD LM LENGTH OF MOMENT EXPANSION;
 CD 0 FOR SCALAR DATA
 CD NRESP NUMBER OF RESPONSES
 CD IFMOM 1 IF RESPONSE OR MOMENT RECORDS
 CD ARE PRESENT
 CD IFBND 1 IF BOUNDARY RECORDS ARE PRESENT
 CD ISOP 1 IF UNCOLLIDED FLUX RECORDS ARE PRESENT
 CD IDUM(I) ARRAY SET TO 0
 C

C-----

C
C

C-----

CR INDEXING ARRAYS

C

CL (IMBIS(IS),IS=1,ISM), (JMBJS(JS),JS=1,JSM),
 CL ((ISET(JNK),J=1,JMS),K=1,KM), (JSET(K),K=1,KM)

C

CW NUMBER OF WORDS= ISM+JSM+JMSKM+KM

C

CD IMBIS(IS) NUMBER OF CELLS IN I-SET IS
 CD JMBJS(JS) NUMBER OF ROWS IN J-SET JS
 CD ISET(JNK) I-SET ASSIGNED TO ROW J IN PLANE K
 CD JSET(K) J-SET ASSIGNED TO PLANE K

C

C-----

C

C

C-----

CR REAL ARRAYS

C

CL ((X(I),I=1,IMSISM+ISM), ((Y(J),J=1,JMSJSM+JSM),

CL (Z(K),K=1,KM+1), (ENER(IG),IG=1,IGM),EMIN,ENEUT,

CL (DAMPG(IG),IG=1,2*IGM)

C

CW NUMBER OF WORDS= IMSISM+ISM+JMSJSM+JSM+KM+3*IGM+3

C

CD X(I) I-INTERVAL BOUNDARIES FOR ALL ISETS

CD Y(J) J-INTERVAL BOUNDARIES FOR ALL JSETS

CD Z(K) K-INTERVAL BOUNDARIES

C

CD ENER(IG) TOP ENERGY BOUNDARY OF GROUP IG

CD EMIN BOTTOM ENERGY BOUNDARY OF GROUP IGM

CD (0 IF NEUT=IGM)

CD ENEUT BOTTOM ENERGY BOUNDARY OF GROUP NEUT

CD (0 IF NEUT=0)

CD DAMPG RESTART ACCELERATION DAMPING DATA

C

C-----

C

C

C-----

CR CELL RESPONSE DATA

C

CL (((CLRES(I,J,K),I=1,IMS),J=1,JMS),K=1,KM)

C

CW NUMBER OF WORDS= SUM OF IMS OVER J AND K

C

CD CLRES CELL-AVERAGE RESPONSE DATA

C

C-----

```

-----
C
C

C-----
-----
CR CELL MOMENT DATA
C
CL ((FLUM(I,L),I=1,IMS),L=1,LM)
C
CW NUMBER OF WORDS= IMS(JNK)*LM
C
CD IMS(JNK)                                NUMBER OF CELLS IN ROW J OF PLANE K
C
CD FLUM                                    CELL-AVERAGE MOMENT DATA
C

C-----
-----
C
C

C-----
-----
CR I-BOUNDARY DIRECTIONAL FLUX
C
CL ZERO
C
CW NUMBER OF WORDS= 1
C

C-----
-----
C
C

C-----
-----
CR J-BOUNDARY DIRECTIONAL FLUX
C
CL ZERO
C
CW NUMBER OF WORDS= 1
C

C-----

```

```

-----
C
C

C-----
-----
CR K-BOUNDARY DIRECTIONAL FLUX
C
CL ZERO
C
CW NUMBER OF WORDS= 1
C

C-----
-----
C
C

C-----
-----
CR UNCOLLIDED FLUX DATA
C
CL ((FLIJ(I,J),I=1,IMS),J=1,JMS)
C
CW NUMBER OF WORDS= SUM OF IMS OVER J
C
CD FLIJ CELL-AVERAGE UNCOLLIDED FLUX DATA
C

C-----
-----
C
C END

```

B.4 QUAD3D Output File Format

Records 1 through 2*nquad:

```
do nq=1,nquad  
  
  qnam(nq),mmq(nq)  
  
  (cosl(m),m=1,mmq(nq)), (cosu(m),m=1,mmq(nq)), (phil(m),m=1,mmq(nq)), (phiu(m),m=1,mmq(nq)),  
  (wts(m),m=1,mmq(nq)), (amu(m),m=1,mmq(nq)), (eta(m),m=1,mmq(nq)), (xzi(m),m=1,mmq(nq))  
  
enddo
```

Notes:

nquad is the number of 3-D quadrature sets on the file (13), qnam(nq) is the 4-character name given to quadrature set nq, and mmq(nq) is the number of directions in quadrature set nq. cosl and cosu are the lower and upper polar cosine boundaries of the 3-D quadrature solid angles, and phil and phiu are the lower and upper azimuthal angle boundaries of the 3-D quadrature solid angles. wts, amu, eta are the quadrature components input to TORT and xzi are the computed y-direction cosines.

B.5 G2GAIR Output File Format

Record 1: (titl(i),i=1,18)

Record 2: jgm, neuto, imo, ism, constm, rref

Record 3: (rout2(i),i=1,imo), (amu2(m),m=1,ism), (wts2(m),m=1,ism), (e3(jgskp+ig),ig=1,jgm+2)

Records 4 through jgm*jgm+3

```
do ig=1,jgm
```

```
do jg=1,jgm
```

```
((xtr(m,i,jg,ig),m=1,ism),i=1,imo)
```

```
enddo
```

```
enddo
```

Notes:

titl is the problem title in 18 four-character words. jgm=igm-jgskp. The elements of the array rout2 are the user-specified output fluence positions less rref, and the arrays amu2 and wts2 are the cosines and weights derived from binning the ANISN quadrature and dropping the zero-weight angle. The xtr array contains the angular fluences at the output spatial locations. neuto=max(neut-jgskp,0). Other parameters are as defined in the input instructions.

B.6 PLATEQ Output File Format

Record 1: (hnam(i),i=1,4)

Record 2: (datex(i),i=1,5), (titl(i),i=1,12)

Record 3: i1, i2, j1, j2, k1, k2, igm

Record 4: (xb(i),i=i1,i2), (yb(j),j=j1,j2), (zb(k),k=k1,k2)

Records 5 through igm+4:

```
do ig=1,igm
```

```
((qs(i,j),i=1,imc),j=1,jmc)
```

```
enddo
```

Notes:

i1, i2, j1, j2, k1, and k2 are the minimum and maximum patch boundary intervals for x, y, and z, respectively. xb, yb, and zb are the midinterval values of x, y, and z. imc=i2+1-i1 and jmc=j2+1-j1. The qs array gives the ground source in the TORT group structure for mesh cells lying within the i and j patch boundaries. The first two records just give character data for file identification.

B.7 VIST3DP Scalar Fluence File Format

This file is used by DRC3SRF or DRC4 (idos=2) to obtain the free-field fluences at specified locations. Fluences are both input from and output to a fixed-mesh file.

Record 1: (hnam(i),i=1,4)

Record 2: (titx(i),i=1,14)

Record 3: igm, im, jm, km, izm, neut, ione, ione, niflx, njflx, nkflx, (izero, i=1,14)

Record 4: ione

Record 5: ione

Record 6: (x(i),i=1,im+1), (y(j),j=1,jm+1), (z(k),k=1,km+1), (aone, n=1,3*igm+2)

Records 7 through km+6:

```
do k=1,km
```

```
ione
```

```
enddo
```

Records km+7 through (igm+1)*km+6:

```
do ig=1,igm
```

```
do k=1,km
```

```
((flx(i,j),i=1,im),j=1,jm)
```

```
enddo
```

```
enddo
```

Notes:

izero=0, ione=1, aone=1.0, niflx=im, njflx=jm, nkflx=km, and flx is the scalar fluence array for plane k and group ig. Other parameters are defined as in TORT. titl is the VIST3DP problem title in eighteen

single-precision words. `titx` is the TORT problem title in nine double-precision words. Note that the variable **`titx`** is as specified in the DOORS description of the "varscl" file format. This format shows nine words of eight characters each. Other file formats show twelve double-precision words with only six characters from the title being stored in each one.

B.8 VIST3DP Directional Fluence File Format

This file contains directional fluences for a fixed mesh. The input file is one that results from the processing of a TORT patch boundary directional fluence file through TORSET. The uncollided and collided fluences are combined and the results are normalized to the total scalar fluences if the data are provided. The uncollided directional fluences are input if needed. They can be reconstructed externally from the uncollided fluence moments. The first and second records of the file are made nearly compatible with the VISTA output file used for DORT-MASH coupling. Therefore, some of the data written are just placeholders.

Record 1: (titl(i),i=1,18),(titx(j),j=6,14)

Record 2: igm, im, jm, km, mm, igp, mmdn, mmup, niflx, njflx, nkflx, jstrt, jlst

Record 3: (xb(i),i=1,im), (yb(j),j=1,jm), (zb(k),k=1,km)

Record 4: (wts(m),m=1,mm), (amu(m),m=1,mm), (eta(m),m=1,mm), (xzi(m),m=1,mm)

Record 5: (cosl(m),m=1,mm), (cosu(m),m=1,mm), (phil(m),m=1,mm), (phiu(m),m=1,mm)

Record 6: (xyzb(i),i=1,6)

Records 7 through 3*igm+6

```
do ig=1,igm
  (((bx(m,j,k),m=1,mm),j=1,jm),k=1,km)
  (((by(m,i,k),m=1,mm),i=1,im),k=1,km)
  (((bz(m,i,j),m=1,mm),i=1,im),j=1,jm)
enddo
```

Definitions:

titl VIST3DP problem title in eighteen single-precision words.

titx TORT problem title in nine double-precision words that are read from the TORSET output file.

igm Number of energy groups.

im Number of x intervals for the TORSET file.

jm Number of y intervals for the TORSET file.

km Number of z intervals for the TORSET file.

mm Number of quadrature directions.

igp $igm+1$

mmdn Number of downward directions in the quadrature set.

mmup Number of upward directions in the quadrature set.

niflxim.

njflxjm.

nkflxkm.

jstrt No meaning here. For VISTA, this is the lower z-interval bounding the target geometry.

jlst No meaning here. For VISTA, this is the upper z-interval bounding the target geometry.

wts Quadrature weights.

amu Quadrature x-direction cosines.

xzi Quadrature y-direction cosines.

eta Quadrature z-direction cosines.

cosl Lower polar cosine boundaries of the quadrature solid angle bins.

cosu Upper polar cosine boundaries of the quadrature solid angle bins.

phil Lower azimuthal angle boundaries of the quadrature solid angle bins.

phiu Upper azimuthal angle boundaries of the quadrature solid angle bins.

xb x-interval midpoint locations where fluences are output.

yb y-interval midpoint locations where fluences are output.

zb z-interval midpoint locations where fluences are output.

xyzbx, y, and z locations of the left, right, inner, outer, bottom, and top boundary surfaces.

bx Directional fluence array for the x-boundary surfaces (one group at a time).

by Directional fluence array for the y-boundary surfaces (one group at a time).

bz Directional fluence array for the z-boundary surfaces (one group at a time).

Note that the variable **titx** is as specified in the DOORS description of the "dirflx" file format. This format shows nine words of eight characters each. Other file formats show twelve double-precision words with only six characters from the title being stored in each one. The optional output TORT boundary fluence file is written in VARBND format.

INTERNAL DISTRIBUTION

- | | | | |
|-------|-----------------|--------|--|
| 1-2. | J. M. Barnes | 11-12. | R. T. Santoro |
| 3. | D. T. Ingersoll | 13-14. | C. O. Slater |
| 4-5. | J. O. Johnson | 15. | Central Research Library |
| 6. | M. A. Kuliasha | 16. | Laboratory Records-RC |
| 7. | R. H. Morris | 17. | Laboratory Records (for
submission to OSTI) |
| 8. | J. V. Pace III | | |
| 9-10. | J. P. Renier | | |

EXTERNAL DISTRIBUTION

18. Dr. Scott Bradley, Logicon Advanced Technology, 6940 S. Kings Hwy., STE 204, Alexandria, VA 22310
19. LTC Todd A. Hann, Defense Threat Reduction Agency, TDACC, 6801 Telegraph Road, Alexandria, VA 22310-3398
20. Mr. Robert Kehlet, Defense Threat Reduction Agency, TDACC, 6801 Telegraph Road, Alexandria, VA 22310-3398
21. Captain Donald Root, Defense Threat Reduction Agency, TDS, 6801 Telegraph Road, Alexandria, VA 22310-3398
22. Dr. Leon Wittwer, Defense Threat Reduction Agency, TDAC, 6801 Telegraph Road, Alexandria, VA 22310-3398